

MAGNETIC ACTUATION, HEAT TRANSFER AND MICROSYSTEM
APPLICATIONS OF IRON-OXIDE NANOPARTICLE BASED FERROFLUIDS

EVİRİM KURTOĞLU

Submitted to the Graduate School of Engineering and Natural Sciences
in partial fulfillment of
the requirements for the degree of
Master of Science

SABANCI UNIVERSITY

MAGNETIC ACTUATION, HEAT TRANSFER AND MICROSYSTEM
APPLICATIONS OF IRON-OXIDE BASED FERROFLUIDS

APPROVED BY:

Assoc. Prof. Dr. Ali Koşar

(Thesis Supervisor)

Asst. Prof. Dr. Burç Mısırlıoğlu

Assoc. Prof. Dr. Devrim Gözüa ık

Assoc. Prof. Dr. Mehmet Yıldız

Asst. Prof. Dr. G zde İnce

DATE OF APPROVAL: 29/05/2013

© Evrim Kurtođlu 2013

All Rights Reserved

MAGNETIC ACTUATION, HEAT TRANSFER AND MICROSYSTEM
APPLICATIONS OF IRON-OXIDE BASED FERROFLUIDS

Evrin Kurtoğlu

Mechatronics Engineering, M.Sc. Thesis, 2013

Thesis Supervisor: Assoc. Prof. Dr. Ali KOŞAR

Keywords: Ferrofluids, magnetic actuation, convective heat transfer, heat transfer enhancements, microsystems, microtubes, minitubes.

ABSTRACT

Ferrofluids are colloidal suspensions, in which the solid phase material is composed of magnetic nanoparticles, while the base fluid can potentially be any fluid. The solid particles are held in suspension by weak intermolecular forces and may be made of materials with different magnetic properties. Magnetite is one of the materials used for its natural ferromagnetic properties. They have vital applications in the field of microfluidics such as microscale flow control in microfluidic circuits, actuation of fluids in microscale, and drug delivery mechanisms. Heat transfer performance of such ferrofluids is also one of the crucial properties among many potential coolants that should be analyzed and considered for their wide range of applications.

In the first study, different families of devices actuating ferrofluids were designed and developed to reveal this potential. A family of these devices actuates discrete plugs, whereas a second family of devices generates continuous flows in tubes of inner diameter ranging from 254 μ m to 1.56mm. The devices were first tested with minitubes to prove the effectiveness of the proposed actuation method. The setups were then adjusted to conduct experiments on microtubes. Promising results were obtained from the experiments. Flow rates up to 120 μ l/s and 0.135 μ l/s were achieved in minitubes and microtubes with modest maximum magnetic field magnitudes of 300mT for discontinuous and continuous actuation, respectively. The proposed magnetic actuation method was proven to work as intended and is expected to be a strong alternative to the existing micropumping methods such as electromechanical, electrokinetic, and piezoelectric actuation. The results suggest that ferrofluids with magnetic nanoparticles merit more research efforts in micro pumping.

In the second study, convective heat transfer experiments were conducted in order to characterize convective heat transfer enhancements with Lauric acid coated ironoxide (Fe₃O₄) nanoparticle based ferrofluids, which have volumetric fractions between 0%- ~5% and average particle diameter of 25 nm, in a 2.5 cm long hypodermic stainless steel microtube with an inner diameter of 514 μm and an outer diameter of 819 μm. Heat fluxes up to 184 W/cm² were applied to the system at three different flow rates (1ml/s, 0.62ml/s and 0.36 ml/s). A decrease of around 100% in the maximum surface temperature (measured at the exit of the microtube) with the ferrofluid compared to the pure base fluid at significant heat fluxes (>100 W/cm²) was observed. Moreover, the enhancement in heat transfer increased with nanoparticle concentration, and there was no clue for saturation in heat transfer coefficient profiles with increasing volume fraction over the volume fraction range in this study (0%-5%). The promising results obtained from the experiments suggest that the use of ferrofluids for heat transfer, drug delivery, and biological applications can be advantageous and a viable alternative as new generation coolants and futuristic drug carriers.

DEMİR-OKSİT BAZLI FERROSIVILARIN MANYETİK EYLEME, ISI TRANSFERİ VE MİKROSİSTEM UYGULAMALARI

Evrin Kurtoğlu

Mekatronik Mühendisliği, Yüksek Lisans Tezi, 2013

Tez Danışmanı: Doç. Dr. Ali KOŞAR

Anahtar Kelimeler: Ferrosivılar, manyetik eyleme, konvektif ısı transferi, ısı transferi iyileştirmesi, mikrosistemler, mikrotüpler, minitüpler.

ÖZET

Ferrosivılar katı fazda manyetik nanopartiküller, sıvı fazda ise herhangi bir baz sıvısının kompozisyonundan oluşan koloid süspansiyonlardır. Katı parçacıklar farklı manyetik özellikteki malzemelerden yapılabilirler ve zayıf moleküller arası kuvvetler ile süspansiyonda tutulurlar. Manyetit doğal ferromanyetik özellikleri sebebiyle kullanılan malzemelerden biridir. Ferrosivılar, mikroakışkanlar alanında, mikroakışkan devrelerinde mikro ölçekte akış kontrolü, akışkanların mikro ölçekte eylemesi ve ilaç sevkiyat mekanizmaları gibi önemli uygulamalara sahiptir. Bu ferrosivıların ısı transferi performansları da diğer bir çok potansiyel soğutucu gibi analiz edilmeli ve geniş kapsamlı uygulama alanları dikkate alınmalıdır.

Yapılan ilk çalışmada, potansiyellerini ortaya çıkarmak amacıyla ferrosivı eyleyen çeşitli cihazlar tasarlandı ve geliştirildi. İki ayrı amaç için tasarlanan bu cihaz gruplarından ilki kesikli sıvı paketleri eylemesi, ikincisi ise iç çapları 254µm'den 1.56mm'ye değişen tüplerde devamlı akış yaratmak üzere tasarlandılar. Tasarlanan cihazlar öncelikle sunulan eyleme metodunun verimliliğini kanıtlamak amacıyla minitüplerde test edildi. Daha sonra düzenekler mikrotüplerle deneylere devam edilecek şekilde ayarlandı. Deneylerden olumlu sonuçlar elde edilmiştir. Minitüpler ve mikrotüplerden maksimum 300mT manyetik alan değerleri ile devamsız ve devamlı akışlarda sırasıyla 120µl/s ve 0.135µl/s'ye kadar akış debileri elde edilmiştir. Sunulan manyetik eyleme metodunun çalıştığı ispatlanmıştır ve elektromekanik, elektrokinetik ve piezoelektrik gibi var olan mikropompalama metodlarına güçlü bir alternatif olabileceği beklenmektedir. Sonuçlar manyetik nanoparçacıklar içeren ferrosivıların mikro pompa uygulamalarında daha fazla araştırma eforu hak ettiğini göstermiştir.

İkinci çalışmada, 2.5 cm uzunluğunda, iç çapı 514 µm ve dış çapı 819 µm olan hipodermik paslanmaz çelik mikrotüp içerisinde, ortalama parçacık çapı 25 nm ve hacimsel fraksiyonları 0%- ~5% arasında olan laurik asit kaplı demir oksit (Fe₃O₄) nano parçacık bazlı ferrosivıların konvektif ısı transferi iyileştirmesini karakterize

etmek amacıyla, konvektif ısı transferi deneyleri yapılmıştır. Sisteme üç farklı akış debisinde (1ml/s, 0.62ml/s ve 0.36 ml/s) 184 W/cm² varak ısı akısı uygulanmıştır. Yüksek ısı akılarında (>100 W/cm²), (mikrotüpün çıkışından ölçüm alındığında) saf baz sıvısına kıyasla maksimum yüzey sıcaklığında 100% civarında azalma gözlenmiştir. Ek olarak, ısı transferindeki iyileştirme nanoparçacık konsantrasyonu ile birlikte artmış ve bu çalışmadaki hacimsel fraksiyon aralığında (0%-5%), artan hacimsel fraksiyonlarda ısı transferi katsayısı profillerinde herhangi bir satürasyona rastlanmamıştır. Deneylerden elde edilen gelecek vaadeden sonuçlar ferrosivilerin ısı transferi, ilaç sevkiyatı ve biyolojik uygulamalarda kullanımının yeni nesil soğutucular ve geleceğin ilaç taşıyıcıları için avantajlı ve geçerli bir alternatif olduğunu göstermiştir.

ACKNOWLEDGEMENTS

I would like to thank my thesis supervisor Dr. Ali KOŞAR for his endless support and guidance throughout my study. His willingness to provide 7/24 help in both academic and life issues gave me the biggest motivation to study at his laboratory. I owe him very much and I hope that I've been a sufficient grad student during my time in Sabanci University.

I send my sincere thanks to my ex-colleague Muhsincan Şeşen and my colleague İlker Sevgen, from whom I have learned a lot, received so much help and advice.

I am very thankful to my thesis committee members Dr. Devrim Gözüaçık, Dr. Burç Mısırlıođlu, Dr. Gözde Özaydın-İnce and Dr. Mehmet Yıldız for giving their precious time for evaluating my MSc thesis.

I also would like to thank to my lab colleagues for their limitless friendship and support. I'd like to thank my colleagues Ebru Demir, Beste Bahçeci, Anastassia Zakhariouta, Soner Ulun and ex-colleague Alp Bilgin especially for their endless help, support and friendship during the entire time I've spent in Sabanci University.

Finally, I would like to thank my family for the constant psychological support and love that they provided.

This study was supported by TUBİTAK (The Scientific and Technological Research Council of Turkey) Support Program for Scientific and Technological Research Projects Grant.

TABLE OF CONTENTS

ABSTRACT.....	1
ÖZET	3
TABLE OF CONTENTS	6
LIST OF FIGURES.....	7
LIST OF TABLES	9
NOMENCLATURE.....	10
1 INTRODUCTION	11
1.1 Literature Survey on Micropumps	11
1.2 Literature Survey on Heat Transfer Enhancement with Ferrofluids.....	14
2 EXPERIMENTAL.....	17
2.1 Overview on Ferrofluid Samples.....	17
2.2 Experimental Setups and Procedures for the Studies of Magnetic Actuation of Iron Oxide Based Ferrofluids.....	18
2.2.1 Operation Principle.....	18
2.2.2 Experimental Setups	22
2.2.3 Theory	26
2.2.4 Uncertainty Analysis.....	28
2.3 Experimental Setup for the Studies of Heat Transfer Enhancement with Ferrofluids.....	28
2.3.1 Experimental Setup.....	28
2.3.2 Data Reduction	30
2.3.3 Uncertainty Analysis.....	31
3 RESULTS AND DISCUSSION.....	33
3.1 Results and Discussions on the Studies of Magnetic Actuation of Ferrofluids.....	33
3.1.1 Rectangular Rotor – Minitube Setup.....	33
3.1.2 Hexagonal Rotor – Minitube Setup.....	34
3.1.3 Rectangular Rotor – Microtube Setup.....	36
3.1.4 Hexagonal Rotor – Microtube Setup.....	37
3.1.5 Conveyor Belt – Microtube Setup.....	37
3.2 Results and Discussion of the Study of Heat Transfer Enhancement with Iron Oxide Based Ferrofluids	38
4 CONCLUSION	48
4.1 Conclusions of the Studies of Magnetic Actuation of Iron Oxide Based Ferrofluids.....	48
4.2 Conclusions of the Study of Heat Transfer Enhancement with Iron Oxide Based Ferrofluids.....	49
4.3 Contribution to the Scientific Knowledge.....	49
REFERENCES.....	51

LIST OF FIGURES

Figure 2.1. DLS Result for Aqueous Solution of SPIONs. Nanoparticle Size Distribution a) Just after Preparation b) 9 Months after Preparation.....	10
Figure 2.2. 1) The magnetized plug is held by two magnets. 2) The rotors rotate slightly to expose the plug to next set of magnets along with the first pair. 3) Rotors fully rotate to move the previous set of magnets away and the magnetized plug. This cycle can be repeated to move the plug in either direction.....	19
Figure 2.3. This schematic visualizes an overly simplified example of skipping. 1) Some of the particles in the fluid are held by a very thin planar magnetic field shown as a line. 2) The moving magnetic field drags the particles, which in turns push the particles in front of them. 3) The magnetic field keeps on moving, but the magnetic force is not enough to force the particles to move through the congestion. The magnetized particles are left behind as the field magnetizes and attracts the closes particles. 4) A new set of particles are fully magnetized, and the magnetic field drags them forward.....	21
Figure 2.4. Rectangular rotor – minitube setup.....	22
Figure 2.5. Hexagonal rotor – minitube setup.....	22
Figure 2.6. Rectangular rotor – microtube setup.....	23
Figure 2.7. Hexagonal rotor – microtube setup.....	24
Figure 2.8. Conveyor belt – microtube setup.....	24
Figure 2.9. a) Experimental Setup, b) Detailed View of the Heated Section (TC: Thermocouple).....	28
Figure 3.1. Flow rate vs angular velocity graph for rectangular rotor – minitube setup.....	35
Figure 3.2. Max. flow rate vs max. magnetic field strength for rectangular rotor – minitube setup.....	33
Figure 3.3. Flow rate vs angular velocity graph for hexagonal rotor – minitube setup.....	34
Figure 3.4. Max. flow rate vs max. magnetic field strength graph for hexagonal rotor setup.....	34
Figure 3.5. Flow rate vs angular velocity for rectangular rotor – microtube setup.....	35

Figure 3.6. Flow rate vs angular velocity for hexagonal rotor – microtube setup.....	36
Figure 3.7. Current vs flow rate graph for conveyor belt set up.....	37
Figure 3.8. Experimental Nusselt number data for pure water.....	38
Figure 3.9. Comparison between the experimental data and existing theory for pure water.....	39
Figure 3.10. Surface temperature rise (with respect to ambient temperature) at a) Q=0.36 ml/s, b) Q= 0.62 ml/s, c) Q=1ml/s.....	40
Figure 3.11. Thermally developing flow.....	42
Figure 3.12. Heat transfer coefficients as a function of applied heat flux at a) Q=0.36 ml/s, b) Q=0.62 ml/s, c) Q=1 ml/s.....	43
Figure 3.13. Heat transfer coefficient enhancement ($h/h_{pure\ water}$) at a) Q=0.36 ml/s, b) Q=0.62 ml/s, c) Q=1 ml/s.....	45
Figure 3.14. Heat transfer enhancement (in %) as a function of dilution amount (with respect to the high concentration nanofluid).....	46

LIST OF TABLES

Table 1.1. Ferrofluid Properties (High Concentration).....	11
Table 2.1. Uncertainty Analysis.....	27
Table 2.2. Uncertainty Data.....	31

NOMENCLATURE

A	Cross Sectional Area, m^2
A_s	Inner Surface Area of the Microtube, m^2
a	Magnet Diameter, m
B	Magnetic Field Strength, T
c_p	Specific Heat Constant, J/K
d	Particle Diameter, m
d_h	Hydraulic Diameter, m
d_i	Inner Diameter of the Channel, m
d_o	Outer Diameter of the Channel, m
F_{mag}	Magnetic Force
F_d	Drag Force
h_{sp}	Single – Phase Heat Transfer Coefficient, $W/(m^2.K)$
i	Magnet Number
k_f	Thermal Conductivity of the Dispersion Liquid, $W/(m.K)$
k_w	Thermal Conductivity of the Microtube Wall, $W/(m.K)$
L	Length of the Magnet Holders, m
Nu	Nusselt number
n	Total Number of the Magnet Pairs
\dot{Q}	Volumetric Flow Rate
\dot{q}	Volumetric Heat Generation
Re	Reynolds Number
T_i	Inlet Temperature, K
$T_{w,i}$	Local Inner Surface Temperature, K
$T_{w,o}$	Local Outer Surface Temperature, K
V	Magnetizable Volume
v	Linear Velocity of Particle
v_{av}	Average Linear Velocity of Particle
x_c	Magnetic Susceptibility of H_2O
x_p	Magnetic Susceptibility of Fe_3O_4

Greek Letters

μ	Viscosity of the Fluid, Pa.s
μ_0	Permeability of Free Space
w	Angular Velocity, rps
ρ	Density of the Magnetic Material, kg/m^3
ΔP	Pressure Drop
Φ	Particle Volume Concentration

1 INTRODUCTION

1.1 Literature Survey on Micropumps

Fabrication of the first literal micropumps has been enabled by the emergence of Microelectromechanical Systems (MEMS) fabrication in the 1980s [1-4] and was followed by the innovatory advances of the actuation methods such as the magnetically actuated ferrofluids. As a result of these developments, the first ferrofluidic piston pump was first offered in 1991 [5]. The realization continued with new developments on the actuation methods such as the electromagnetically actuated ferrofluidic micropipette [6], magnetic actuation and valving application of ferrofluidic plugs [7-8]. With the developing MEMS technology, existing micropumps vary in complexity and effectiveness but the most important aim in micropump designs is to achieve simple yet effective micropumps that could be easily combined with other microfluidic elements to have portability [9].

Magnetic actuation of ferrofluids is becoming a very popular research area with its wide and differing application areas such as biomedical [10-11], microelectronics [12], microelectromechanical systems (MEMS) [13] and biological microelectromechanical systems (bioMEMS) applications [14-15]. In micropumping applications, it is necessary to use magnetic actuation with non-uniform magnetic field strength gradients since significant flow rates can be achieved with this method [16] without tactile interference with the fluid flow. Nanofluids for this task are colloidal compounds, where the solid phase material is composed of nano sized particles, while the liquid phase can potentially be any fluid, but aqueous media are common. The solid particles are held in suspension by weak intermolecular forces. The particles may be synthesized from materials with different magnetic properties [17]. Magnetite (Fe_3O_4) is one of the well-known materials used for its natural ferrimagnetic properties. It has a spinel structure where oxygen ions sit on the corners of a cube and there appear tetrahedral and octahedral sites available for Fe ions. Fe has two oxidation states at tetrahedral and octahedral sites: Fe^{+2} at tetrahedral sites and Fe^{+3} at octahedral sites. The sign of the exchange interaction between the two Fe sites is a negative and therefore spin alignment is antiparallel. However, the spin moments are not equal and a net moment from the Fe^{+2} sites remains uncanceled, creating the net permanent magnetic moment density in the crystal. Magnetite has a significant susceptibility to external

magnetic fields and is easy to synthesize, making it one of the favored materials for magnetic fluids. A magnetite-based ferrofluid could be moved with magnetic fields, which makes magnetic manipulation a possibility.

For magnetite based nanofluids, each particle is desired to be sufficiently small so that it will exist in the superparamagnetic limit, where each particle consists of a single magnetic domain. Depending on the extent of the anisotropy energy in such systems and the surface area-to-volume ratio magnetic poly domains can significantly reduce the response of the particles to external applied fields. Synthesizing these particles with sizes comparable or smaller than the domain wall widths (at the order of 50-100 nm) stabilizes a material that is in the superparamagnetic limit and can have a strong linear response to external fields without any undesired hysteresis effects. Such magnetic particles in the superparamagnetic limit can be suspended in the fluid and can be magnetized through an external magnetic field's influence [18]. The magnetized particles move to saturate the magnetic field, and thus, a ferrofluid plug is formed. The existence of a magnetic field is also expected to change the viscous properties of the composite fluid [16].

Ferrofluids retain their fluid characteristics even under strong magnetic forces. Carefully engineered ferrofluids return to initial diffusion state at the moment of demagnetization without any irreversibilities for many magnetization cycles [19]. Surfactants are an integral part of the nanofluids, which provide the longevity and stability of the fluids. Particles must be covered with surfactants to prevent agglomeration of particles and to help retain the colloid state [20]. The function and amount of surfactants in fluids can be engineered according to their application [21]. The emergence of ferrofluids brought up the possibility of implementing magnetic actuation in fluidic and hydraulic systems. The novel advantage of non-tactile actuation is open to exploitation [22]. Microscale application of magnetic fields in fluidic applications requires the efficient generation of magnetic fields to improve power management and to prevent undesirable interactions [23]. Optimization of magnetic field topologies in theoretical realm is trivial, yet realizing some of the most optimal designs in real world can be considered as unusual feats of engineering.

While magnetic actuation of ferrofluids in microchannels has not received significant attention in the microfluidics community yet during the last decade, the advantages offered by this intelligent magnetic actuation are various. Magnetic actuation allows fine control of magnetic particles in a non-magnetic medium and

mostly ignores the charges, pH values and moderate temperature variations [19, 24]. Currently, magnetic actuation is an expanding research field that offers different approaches and solutions and is implemented in the microfluidics context. Fine magnetic manipulation of particles and specimens labeled with magnetic indicators was proven to be possible [25-26]. Through the use of ferrofluid plugs, non-ferrous fluids were also indirectly actuated with magnetic manipulation [19, 27]. Although magnetic actuation is freely scalable, smaller physical scales allow better efficiencies. Objects ranging from nano scale magnetite crystals to micro scale biological specimens can be treated with magnetic actuation methods. This kind of actuation is being continuously articulated, and the achievable finesse is being continuously improved [26].

Advances in microfluidics significantly improved biotechnological and medical processes. Sample volumes, costs and consumption of hazardous materials are decreased, whereas portability and integrability are improved. Delicate manipulation of bio-matter of micro-nano scales is a prerequisite of improving biological application of microfluidics [23]. Development of new pumping methods directly improves technologies related to biomedical applications such as diagnostics, drug delivery and lab-on-chip [28-30]. Reliability, device compatibility and biocompatibility are improved via engineered materials and novel actuation methods [24].

Samples which are frequently used as materials for nano particles, such as iron oxides, are mostly bioresorbable [18]. Their usage in biomedical applications and chemical analysis systems are therefore not restrained. Since very high power permanent magnets and very small scale inductors are readily available, development of systems that utilize these materials is not expected to be as prohibitively expensive [31].

Microfluidic control structures that employ magnetic forces as the primary mode of actuation can realistically be designed and implemented. Magnetizable fluids can be pumped or held in place with varying magnetic fields. Processing of magnetic or non-magnetic objects travelling in the fluid is possible with this technique [32-34].

Plug magnetization of fluids is one viable method of realizing pumping systems. These systems are driven by externally generated magnetic fields. This idea simplifies the device designs and decreases production costs. Magnetized fluid plugs can actuate other non-magnetic fluids, given that the two fluids do not mix [19,27].

Motivated by the aforementioned studies and findings, in order to provide more insight into magnetic actuation of ferrofluids in mini/micro scale, the first study focuses on the development of pumping devices that operate with the principle of ferrofluid

actuation with varying magnetic fields. The objective is designing a compact device that utilizes permanent magnets to actuate ferrofluids. Ideally, the pumping method is exploited in such a way that it would be applicable to discrete and continuous actuations. Two groups of devices were utilized for this purpose. A family of devices actuated discrete ferrofluid plugs, whereas a second family of devices generated continuous ferrofluid flows. The devices were first tested with 1.56mm inner diameter minitubes to prove the effectiveness of the proposed actuation method. The setups were then adjusted for the tests with 254 μm inner diameter microtubes.

1.2 Literature Survey on Heat Transfer Enhancement with Ferrofluids

Heat transfer in microchannels has become progressively important with the rapid development of microelectronic devices and micro manufacturing technology, since microchannel heat exchangers and evaporators present several advantages, such as reduced size, higher thermal efficiency and low fluid inventory. Therefore numerous solutions have been proposed over decades for enhancing heat transfer performances of thermal devices. Maximizing heat transfer area and increasing the convective heat transfer coefficients were the most commonly used solutions. As for maximizing the heat transfer area in heat exchangers with the recent technology and developments, no further developments could be achieved at the moment consequently, since convective heat transfer can be enhanced passively by changing flow geometry, boundary conditions, or by enhancing thermal conductivity of the fluid, improving the characteristics of the traditional working fluids such as water, glycol, oil and refrigerants, have also been tried in order to increase the thermal conductivity of base fluids by suspending micro- or larger-sized solid particles in fluids, as the thermal conductivity of solid is typically higher than that of liquids. Numerous theoretical and experimental studies of suspensions containing solid particles have been conducted since Maxwell's theoretical work was published in 1881 [35]. Yet, due to the large size and high density of the particles, it is not possible to prevent the solid particles from settling out of suspension and the lack of stability of such suspensions induces additional flow resistance and possible erosion. As a result, with the modern nanotechnology, which provides new opportunities to process and produce materials with average crystallite sizes below 50 nm, a new research area has emerged with the

new generation of thermal vectors which are called nanofluids to find an alternative method for enhancing heat transfer [36-39].

Nanofluids, which are the new kind of heat transfer medium, containing uniformly and stably distributed nanoparticles in a base fluid, were first proposed in 1995 [40]. It is well known that distributed nanoparticles with high thermal conductivity greatly enhance the thermal conductivity of the nanofluid compared to pure liquids. Therefore they are expected to have superior properties compared to conventional heat transfer fluids, as well as fluids containing micro-sized metallic particles. The much larger relative surface area of nanoparticles, compared to those of conventional particles, should not only significantly improve heat transfer capabilities, but also should increase the stability of the suspensions. Also, nanofluids can improve abrasion-related properties as compared to the conventional solid/fluid mixtures. It was showed that when a small amount of nanoparticles and nanotubes is added, the enhancement of the thermal conductivity of base fluids of ethylene glycol and oil could reach up to 160% [41-42]. As reported in recent studies, Brownian motion and the convective motion driven by thermal gradient (thermophoresis) have significant effect on heat transfer enhancement with nanofluids in a pool [43-44]. In addition, successful employment of nanofluids will support the current trend toward component miniaturization by enabling the design of smaller and lighter heat exchanger systems. As a result, nanofluids, which include the suspension of nanoparticles within the range of 1-100nm, have become a popular research topic in heat transfer enhancement [45-48] and are being utilized in a large variety of applications such as engine cooling, refrigeration, lubrication, and thermal storage [49-54]. As a type of nanofluids, ferrofluids have also received attention and been utilized in numerous promising application areas such as biomedical [10, 28, 55], microfluidic [6, 9, 23, 56], microelectronic [12, 13, 29, 57] and microelectromechanical systems [14-15] applications.

Ferrofluids are magnetic colloidal suspensions consisting of carrier liquid and magnetic nanoparticles with a size range of 1 to 100 nm in diameter coated with a surfactant layer. The most often used magnetic material is single domain particles of magnetite, iron, or cobalt; and the carrier liquids such as water or kerosene. Ferrofluids are different from the usual magnetorheological fluids (MRF) which are formed by micron sized particles dispersed in oil. In MRF, the application of a magnetic field causes an enormous increase of the viscosity, so that, for strong enough fields, they may

behave like a solid. On the other hand, ferrofluids keep its fluidity even if subjected to strong magnetic fields. One of the many advantages of the ferrofluids is that the fluid flow and heat transfer can be controlled by an external magnetic field which makes it applicable in the previously mentioned areas. In addition to the macroscopic applications, there are plenty of promising applications in MEMS for the ferrofluids. As examples; mesoscopic models have been developed to simulate the magnetic fluid flowing through a microchannel in the presence of a magnetic field gradient using the lattice-Boltzmann method [58], actuators were developed by using ferrofluids [59-60] for a ventricular assist device or for liquid dispensing in microfluidic channels, magnetocaloric pumping was studied for microfluidic applications [9, 61].

Heat transfer is one of the crucial topics for the utilization of ferrofluids, in which ferrofluids have many advantages over the conventional commonly used fluids such as water, oil or air. Ferrofluids contain colloidal suspensions with outstanding magnetic properties, and their solid nanoparticles have the advantage of offering high thermal conductivity at the same time. Moreover, their nano-size particles (in this study 25 nm average diameter) are more stable and could prevent clogging the mini/micro channels [35, 62-63]. Another specific advantage ferrofluids only have is their ability to be manipulated to the desired point with magnetic field gradients [64-66]. Indeed, ferrofluids were magnetically manipulated for biomedical treatment purposes allowing them to target diseased tissues and organs in a more focused and specific fashion [67].

As a continuation of research efforts in this field, in this second study, convective heat transfer performances of the lab-made SPION samples were investigated at different concentrations, flow rates and different power values applied to the experimental test section.

2 EXPERIMENTAL

2.1 Overview on Ferrofluid Samples

A lab-made sample of Lauric acid-coated super paramagnetic Iron oxide (SPIO-LA) was used as the ferrofluid species in these studies. SPIO-LA has magnetic nano particles, which have 25 nm average diameter. The fluid is prepared by co-precipitation of aqueous solutions of FeCl_2 and FeCl_3 in a basic environment. Through fine control of the addition rate of the reactants to the reaction vessel; considerably small and uniform particle sizes are easily achieved. To prevent aggregation and to facilitate their motion inside the liquid, nanoparticles of SPIO were coated with lauric acid, which also contributes to the long-term stability of the nanofluid.

The sizes of the ferromagnetic nanoparticles in the sample SPIO-LA are 20–30 nm. This refers to the hydrodynamic size in water measured by dynamic light scattering (DLS) and reported as number average. Figure 1 shows the DLS results of the ferrofluid sample, which was used throughout the experiments. As can be seen from Figure 1.1., these aq. SPIONs (Super Paramagnetic Iron Oxide Nanoparticle) are colloiddally stable since they were suspended well-dispersed in the aqueous medium for over a year (even more). Besides, their hydrodynamic sizes measured by DLS on the day of the synthesis and after 9 month indicated no significant change over time again indicating their stability. Their response to an external magnet did not change either.

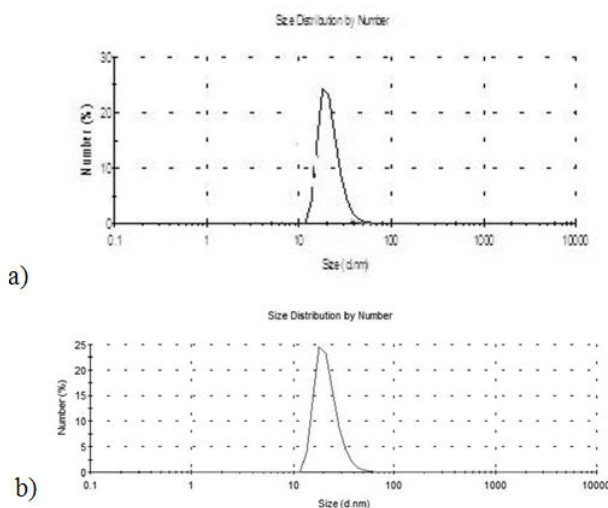


Figure 2.1. DLS Result for Aqueous Solution of SPIONs. Nanoparticle Size Distribution a) Just after Preparation b) 9 Months after Preparation

Forty-five milliliter of distilled water was put into a 100-ml three-necked round-bottom flask fitted with a mechanical stirrer and a condenser and deoxygenated for 30 min. 2.162 g $\text{FeCl}_3 \cdot 6\text{H}_2\text{O}$ and 0.795 g $\text{FeCl}_2 \cdot 4\text{H}_2\text{O}$, lauric acid (LA) were added to the flask and stirred at 400 rpm under nitrogen for about 15 min. Reaction flask was placed in an oil bath at 85 °C. After 10 min of mixing, 7 ml ammonium hydroxide was injected into the flask with vigorous stirring at 600 rpm. Reaction was allowed to continue for 30 min to produce a stable colloidal solution, then cooled to room temperature, and placed atop a magnet (0.3 Tesla) for few hours. Any precipitate was removed with magnetic decantation. Usually, there are no precipitates. Final ferrofluid has 29 mg Fe/l. Further details of the ferrofluid sample used in this study are shown in Table 1.1.

Table 1.1. Ferrofluid Properties (High Concentration)

ID	[Fe] (M)	Si/Fe (mole %)	Base/Fe (mole %)	Dh-I (nm)	Dh-I washed (nm)	Dh-N (nm)	Dh-N washed (nm)
SPIO-LA	0,175	1,25	1,5	23-100	23	32-100	28

2.2 Experimental Setups and Procedures for the Studies of Magnetic Actuation of Iron Oxide Based Ferrofluids

2.2.1 Operation Principle

The presence of a non-uniform magnetic field induces a force on magnetized particles. The particles migrate to the point, where the field is the strongest [68]. Static magnetic fields are capable of agitating ferrofluids, but the fluid quickly falls to equilibrium [69]. Disturbing the equilibrium state by changing the magnetic field is vital, if a useful actuation method is to be developed [27].

To realize a dynamic magnetic field, either stationary sources of variable magnetic power, or moving sources of constant magnetic power can be utilized [4, 27, 61]. Magnetic fields generated by solenoid inductors can be adjusted through electrical systems so that Helmholtz coils placed along the sides of the channel can be used to actuate the fluid. Another approach is mechanically actuating permanent magnets to vary the magnetic field strength.

It was experimentally determined that miniscale inductors fail to generate magnetic fields that are sufficiently strong to compete with extant devices.

A magnetic field, sustained by a permanent magnet, forces the surrounding particles to move towards the magnet surface. When such a field performs a translational motion, it causes a net displacement of particles along the motion direction. In the case of a ferrofluid, the particles are suspended in a viscous fluid medium. If the magnetic force is strong enough, the displaced particles would drag the fluid along the magnetic field's motion direction. If fluid is placed in a channel and magnetic field gradient is placed in parallel or coincident to the channel, the fluid can be forced to move along the channel.

The magnetic field magnetizing the sample fluid must be generated to perform a translation motion parallel to the channel. Constructing a mechanism to perform this task is possible, but the prospects they present towards miniaturization are weak. Mimicking the translational motion of magnets with rotating magnets is a viable solution to this problem. Thus, the problem changes to finding a method of mimicking the resultant magnetic field of a translating magnet with rotating magnets.

The proposed methods in this thesis consist of placing magnets around solid rotors in a spiral pattern. When the rotors are rotated in unison from a starting configuration of a magnet pair facing each other, the magnet pairs periodically face each other. Then the fluid plug reaches the middle point of a magnet pair. They must be disengaged and another pair of magnets is brought in position just in front of the plug so that the plug will move forward. Given that the transitions are smooth and magnetic field is sufficiently strong, the fluid can be smoothly actuated with this technique.

The dynamic behavior of the magnetic field generated by the rotating magnets is inspired by a natural phenomenon. The motion and the shape change of our proposed magnetic field topology resemble the motion of an inchworm. Initially, the magnetic field strength distribution constitutes a single wave, as depicted in Figure 2.2.. The axial coverage of the magnetic field expands by one wavelength towards the intended flow direction, and the peak magnetic field strength simultaneously decreases. Meanwhile, the magnetized plug moves half the field expansion distance. In one continuous motion, the magnetic field begins to contract in the same direction as the expansion, and the field strength increases in a reversal of the previous change, which pushes the fluid yet again for a distance equal to half of the contraction length being also equal to one wavelength. The magnetic field resumes to its initial state only one wavelength away

from the initial position. In this thesis this peculiar dynamic behavior will be called “creep dynamics”.

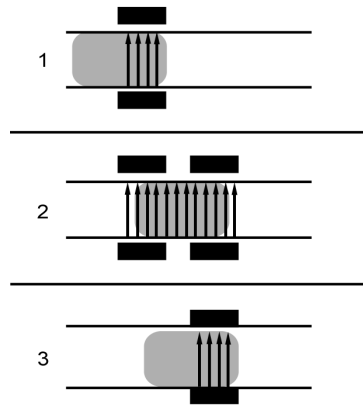


Figure 2.2. 1) The magnetized plug is held by two magnets. 2) The rotors rotate slightly to expose the plug to next set of magnets along with the first pair. 3) Rotors fully rotate to move the previous set of magnets away and the magnetized plug. This cycle can be repeated to move the plug in either direction.

The magnetic force on the ferrofluid is generated by the magnetic field gradient perpendicular to the magnetic field direction in this context. The magnetic force depends on the magnetic field gradient vector. Due to the interactions between the varying magnetic field and its gradient, a horizontal force along the tube is generated so that the plug could move along the tube. This configuration allows generated field sinks and sources to be forced around the tube and thus results in a more compact design.

There are two approaches for the actuation of ferrofluids using magnetic fields. The direct methods that depend on the influence of field over fluid either utilize the discrete magnetization of a plug or produce a homogenous flow induced by the magnetized volume.

The characteristics of the described creep dynamics are beneficial to the actuation of discrete plugs. The semi-discrete magnetization methods employ the non-newtonian properties of the subject fluid with respect to changing magnetic field strength around the fluid [70]. The ferrofluid plug can be pinned to a specific location in the channel by the proposed mechanisms. Implementations of devices that exaggerate the inchworm motion are straightforward, but their practicality is limited to low power applications. This approach yields a discontinuous actuation that is used for

microfluidic valves [70], liquid pistons for pumps [2] and precision actuators for other fluids [6].

The semi-homogenous force methods focus on the design of the magnetic field to induce sufficiently equal forces on multiple plugs. The implementation is tricky but the flow can be continuous [71]. This yields a continuous actuation that is useful when the ferrofluid needs to be pumped as bulk or when it needs to be circulated. The creep dynamics hinders the continuous actuation if the variations of magnetic field are too great. The field variations decrease the efficiency of the pump as the difference gets greater. The characteristics of the creep dynamics must be minimized to achieve a more stable magnetic field.

For both cases the mechanical behavior of the magnetized plug resembles a first order linear differential system. The movement induced by the magnetic force is dampened by the drag forces, and in theory, it reaches a steady state velocity. However, the magnetic force is not constant, shifts in space and changes in magnitude. As a result, the velocity of the fluid is not constant. With continuous actuation, this simply results in a loss of efficiency and maybe degradation of a subjective flow quality. Depending on the application, both could be forgivable. In discontinuous actuation when the fluid fails to track the shifts in the magnetic field it simply remains in the last position until the magnetic field peak comes close again, when the plug moves slightly backwards before moving forwards. This phenomenon is referred as “skipping” in this study as shown in Figure 2.3.

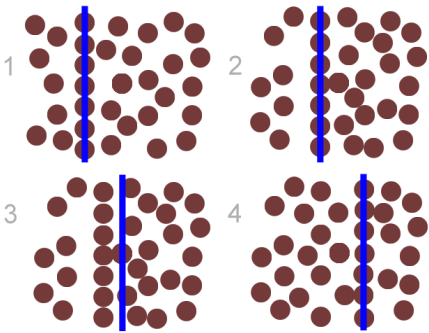


Figure 2.3. This schematic visualizes an overly simplified example of skipping. 1) Some of the particles in the fluid are held by a very thin planar magnetic field shown as a line. 2) The moving magnetic field drags the particles, which in turn push the particles in front of them. 3) The magnetic field keeps on moving, but the magnetic force is not enough to force the particles to move through the congestion. The magnetized particles are left behind as the field magnetizes and attracts the closest particles. 4) A new set of particles are fully magnetized, and the magnetic field drags them forward.

Skipping error is more noticeable if the plug is used in positioning or valving applications, while skipping appears as a loss of pumping power in continuous flow applications.

2.2.2 Experimental Setups

2.2.2.1 *Discontinuous Actuation*

Moving a magnetic field without distorting its shape is trivial if the source of magnetic field can be moved in the same direction. It was decided that such a mechanism would be cumbersome at best. Instead, the linear movement of the magnet was mimicked with magnets rotating around a common axis.

2.2.2.1.1 Minitube Setups

2.2.2.1.1.1 Rectangular Rotor – Minitube Setup

The idea behind this design is using the synchronous rotation of symmetric and opposing magnets to generate a magnetic field, which peaks, when the magnets are at the closest position, and which diminishes, while the magnets are at the farthest position. Rare earth magnets with 300mT magnetic field strength are placed on to the each face of the square profile rotors with the $(i-1) \times a$ mm distance from the reference edge, where i is the magnet number and a is the magnet diameter. The rotors are placed in such a way that the tube, which has 3 mm outer diameter, stays in between the rotors, which are actuated by a simple DC motor. The flow rate is obtained by visualizing the motion of plugs using a CCD camera with time. A digital rendering for the setup can be seen in Figure 2.4.

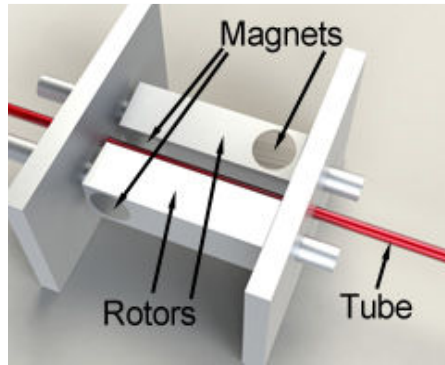


Figure 2.4. Rectangular rotor – minitube setup

Angular velocities are calculated from the position data, which are obtained from the encoder of the motor.

2.2.2.1.1.2 Hexagonal Rotor – Minitube Setup

The previously mentioned pump design could actuate ferrofluid plugs but irregularities were observed on the generated magnetic field, which affected the maximum performance of the pump. Thus, the first design has been improved by reducing the angular separation of rare earth magnet pairs to obtain higher flow rates, fewer discontinuities on the magnetic field and better position tracking. This was achieved by changing rectangular rotors into hexagonal rotors. The improved second setup can be seen in Figure 2.5.

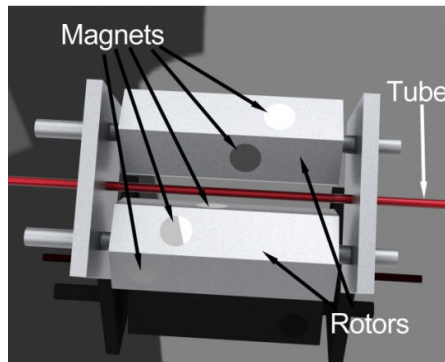


Figure 2.5. Hexagonal rotor – minitube setup

The improvement mentioned above increases the flow rate values of this pump architecture. A comparison of results will be included in the following sections.

2.2.2.1.2 Microtube Setups

2.2.2.1.2.1 Rectangular Rotor – Microtube Setup

Since the ultimate aim is to produce microfluidic devices that can actuate ferrofluids, the next step is to use microtubes. The microtubes used in experiments have 254 μm inner diameter and 762 μm outer diameter. Rectangular rotor setup was modified accordingly for microtube experiments. A digital rendering of the setup can be seen in Figure 2.6.

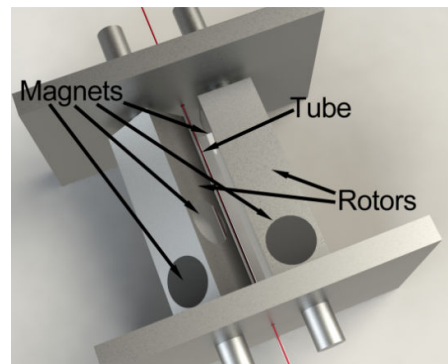


Figure 2.6. Rectangular rotor – microtube setup

2.2.2.1.2.2 Hexagonal Rotor – Microtube Setup

The experiments of inducing flow in microtubes were repeated in the hexagonal rotor setup. A digital rendering of the hexagonal setup with microchannel can be seen in Figure 2.7.

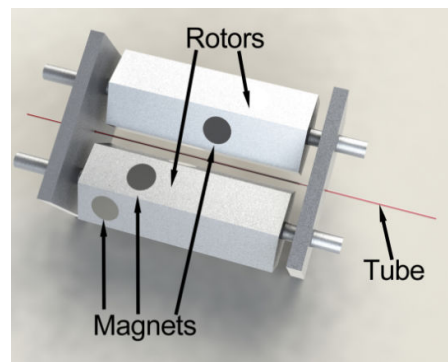


Figure 2.7. Hexagonal rotor – microtube setup

It was seen that contrary to the results seen in mini scale, flow rate values deteriorate for the same angular velocity values in microscale due to size effects of smaller size. The idea of changing the angle between two magnets to improve rectangular rotors is not applicable when it comes to microtubes. The details of corresponding will be explained in Results section.

2.2.2.2 *Continuous Actuation*

After plug actuation methods are studied, the next step is the generation of continuous flows with ferrofluid.

2.2.2.2.1 Conveyor Belt – Microtube Setup

This design is constructed from a conveyor belt, on which rare earth magnets are attached, and two pulleys, which are fixed to two individual shafts that fit into bearings. A gear is affixed to one of the shafts, while another gear is affixed to a DC torque motor. The gears are placed to stay in mesh and the motor is switched on to actuate the mechanism. A simplified digital rendering can be seen in Figure 2.8.

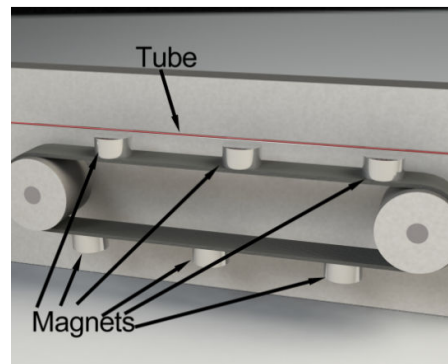


Figure 2.8. Conveyor belt – microtube setup

When current is supplied to the motor, the conveyor belt rotates the magnets so that the ferrofluid could be actuated, and a continuous flow is induced.

The pressure drop of the pump is expected to vary almost linearly between zero difference and the eventual upper limit. Both ends of the microchannel are sealed into graded containers. The fluid flow causes a height difference between the fluid levels in the containers until the flow and the pressure equalize and height difference settles. The height difference between containers can be measured to calculate the exact pressure drop created by the pump.

2.2.3 Theory

Particle based approach can be implemented to explain the theory behind magnetic actuation. For this, a unit cell is constructed as a single particle and an appropriate fraction of the carrier fluid. The forces acting on the magnetic nanoparticle are the magnetic force, F_{mag} , and drag force, F_d , so that Newton's Second Law could be expressed as:

$$m\mathbf{a} + \mathbf{F}_d = \mathbf{F}_{mag} \quad (1)$$

The magnetic force is calculated through the subtraction of the total forces exerted to environment and forces exerted on the particle, where x_c and x_p stand for the magnetic susceptibility of the base and particle. Their difference is multiplied with magnetizable volume, V , and the gradient of the applied magnetic field squared, ∇B^2 , and divided to permeability of free space, μ_0 , to give the magnetic force on a single particle:

$$\mathbf{F}_{mag} = \frac{(x_p - x_c)V\nabla B^2}{2\mu_0} \quad (2)$$

The drag force is found using a generalized drag force acting on a small particle for a low Reynolds number flow due to the small particle size, where μ is the viscosity of the base fluid, v and d are velocity and diameter of the particle, respectively:

$$\mathbf{F}_d = 3\pi\mu\mathbf{v}d \quad (3)$$

The local velocity of the magnetic nanoparticle is deduced from Eqn. 1 by integrating the acceleration over time. An analytical solution for the local velocity is possible under uniform magnetic field gradient assumption and is expressed as:

$$\mathbf{v} = \mathbf{v}_0 e^{-c_1 t} + \frac{c_2}{c_1} (1 - e^{-c_2 t}) \quad (4)$$

where v_0 is the initial particle velocity, $c_1 = \frac{3\pi\mu d}{m}$, and $c_2 = \frac{(x_p - x_c)V\nabla B^2}{2m\mu_0}$

Since moving nanoparticles having high concentration in the base fluid could push the molecules of the base fluid, a bulk fluid flow could be generated. The corresponding volumetric flow rate could be approximated as the product of the average linear velocity of the nanoparticle, v_{av} , and cross sectional area, A :

$$\dot{Q} = v_{av}A \quad (5)$$

The above equations provide a basis for explaining the experimental results. Same magnets are utilized along the both micro and mini tubes, while they would produce similar local magnetic fields and gradients along the channel for the discontinuous actuation configuration. Based on the performed magnetic field measurements by using Teslameter and due to the smaller spacing between the magnets, magnetic field gradients in discontinuous actuation are measured to be around 2.5 times greater than the continuous actuation, while the magnetic susceptibilities are fixed for all the configurations due to the use of the same fluid sample. As a result of greater magnetic field gradients, the magnetic forces are expected to be greater in discontinuous actuation compared to continuous actuation according to Eqns. (2), (4), and (5). As a result, considerably lower flow rates are apparent for continuous fluid actuation compared to discontinuous actuation in microtubes of the same dimension.

When the flow rates of discontinuous actuation are considered, a significant increase in flow rates can be observed when the tube diameter is increased. Since similar magnetic fields and gradients are expected for both minitubes and microtubes similar average velocities will be also obtained for nanoparticles. According to Eqn. 5, the volumetric flow rates should be much larger in minitubes because of the larger inner diameters of minitubes compared to microtubes tested in this study (more than 5 times), which bolsters the experimental findings. In addition to this effect, wall shear stress on the wall also increases for bulk fluid flow with the reduction of the tube diameter leading to a further decrease in the flowrate. As a result, a reduction of more than 100 times in flow rates occurs when switching from minitubes to microtubes.

The position of magnets is adjusted in such a way that plugs could be propelled one by one by placing the first set of two magnets sufficiently close to each other while positioning the other set of two magnets further to the first set. However, for the continuous actuation, it was made sure that each magnet is placed close to each other

and is moved completely horizontally along the entire microtube so that each piece of the working fluid could be continuously driven along the microtube thereby assuring a continuous actuation.

2.2.4 Uncertainty Analysis

The uncertainties in the measured values are given in Table 2.1. They were provided by the manufacturer's specification sheet, whereas the uncertainties on volumetric flow rate and angular velocity were obtained using the propagation of uncertainty method developed by Kline and McClintock (1953) and ISO Guide to the expression of uncertainty [72-73]. Moreover, each measurement of each setup was repeated for ten times and the results were averaged.

Table 2.1. Uncertainty Data

Parameter	Uncertainty (±)
Area	0.94%
Length	0.01%
Volumetric Flow Rate	2%
Angular Velocity	8%
Current	0.01%
Magnetic Field Strength	2%

2.3 Experimental Setup for the Studies of Heat Transfer Enhancement with Ferrofluids

2.3.1 Experimental Setup

The experimental setup consists of a syringe pump with a control unit, microtube test section, temperature sensors integrated to the system, and Data Acquisition system. A syringe pump is built from a linear motor to be able to obtain desired flow rates and

continuous flow of ferrofluid. 2.5 cm long hypodermic stainless steel microchannel, which has inner and outer diameters of 0.514 mm and 0.819 mm, respectively, is used as the heated length. One K-type thermocouple is placed using OmegaBond on the surface at the outlet of the microtube and connected to the Data Acquisition system, from which the temperature values are obtained. A digital rendering of the experimental setup can be seen in Figure 2.9.

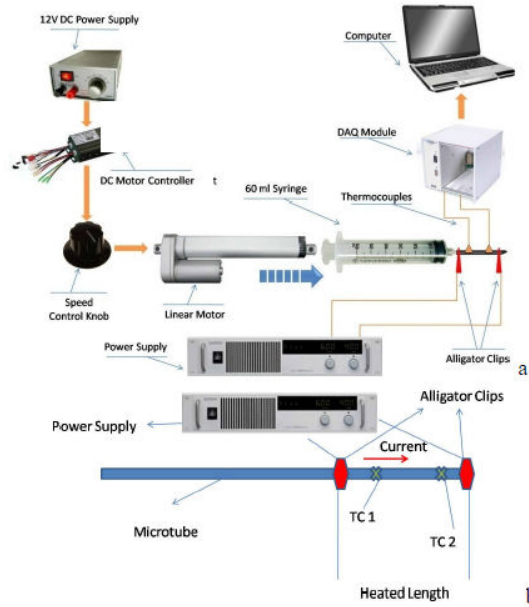


Figure 2.9. a) Experimental Setup, b) Detailed View of the Heated Section (TC: Thermocouple)

A Syringe pump with a Wuxi Hongba HB-DJ809 12V DC linear motor is set to flow rates of 0.36, 0.62 and 1ml/s during the experiments. A *Xantrex XFR20-130* power supply is used to apply desired power values to the test section with alligator clips, and six different power values are constantly applied on each data set corresponding to a different sample of the working fluid. Each data set is obtained under steady state conditions. Heat transfer performances of corresponding fluid samples are obtained with respect to the outlet surface temperature rise which has the highest value in the heated region. For the temperature measurements, Omega® K-Type thermocouples are used, and the thermocouple readings are transferred to the Data Acquisition System for data reduction along with current, voltage and flow rate data. The effects of flowrate and nanoparticle concentration on heat transfer performance of ferrofluids are investigated throughout 12 different data sets with each of them having 6 different input power values. Experiments are conducted under three different concentrations of ferrofluid and

DI (deionized) water mixture. Each data set is tested under steady state conditions, and the experiments were repeated for five times for each set.

2.3.2 Data Reduction

The data obtained from the voltage, current, flow rate, and temperature measurements were used to obtain the single-phase heat transfer coefficients and Nusselt numbers.

Reynolds number is expressed as:

$$Re = \frac{Q}{\mu A_c} d_i \quad (6)$$

where Q is the flowrate, A_c is the microtube cross-sectional area, and d_i is the microtube inner diameter.

The electrical input power and resistance are calculated using the measured voltage and current values. Assuming 1-D steady state heat conduction with uniform heat generation, the local inner surface temperature of the microchannel, $T_{w,i}$, is expressed in terms of the measured local outer surface temperature, $T_{w,o}$, as:

$$T_{w,i} = T_{w,o} + \frac{\dot{q}}{4k_w} (r_o^2 - r_i^2) - \frac{\dot{q}}{2k_w} r_o^2 \log \frac{r_o}{r_i} \quad (7)$$

where k_w is heat thermal conductivity of the wall, r_o is outer radius of the channel, r_i is inner radius of the channel, and \dot{q} is the volumetric heat generation. \dot{q} is expressed as a function of net power P_{net} , inner radius, outer channel radius, and heated length as:

$$\dot{q} = \frac{P_{net}}{\pi(r_o^2 - r_i^2)L_h} \quad (8)$$

Single-phase heat transfer coefficient h_{sp} is calculated using the inner wall temperature and net power as:

$$h_{sp} = \frac{P_{net}}{A_s(T_{w,i} - T_f)} \quad (9)$$

where A_s is inner surface area.

Exit fluid temperatures are deduced from energy balance:

$$T_f = T_i + \frac{P_{net}}{Q\rho c_p} \quad (10)$$

where T_i is inlet temperature, and c_p is specific heat. Finally, Nusselt number of the pure fluid is found using the local heat transfer coefficient as:

$$Nu = \frac{h_{sp}d_i}{k_f} \quad (11)$$

where h_{sp} is single-phase heat transfer coefficient, and k_f is thermal conductivity of the fluid. Since fluid flows were mostly considered as thermally developing flows under the conditions of the present study, the thermally developing flow correlation proposed by Shah and London [74] for laminar flows ($Re < 2300$) was chosen for the comparison with the experimental data obtained from the experiments with pure water. For the turbulent flow portion of the experimental data for pure water, the correlations proposed by a turbulent flow correlation with modifications for developing flows [75] were employed for comparison.

2.3.3 Uncertainty Analysis

The uncertainties in the measured values are given in Table 2.2. Uncertainty values were provided by the manufacturer's specification sheet, whereas the uncertainties on heat transfer coefficients were obtained using the propagation of uncertainty method developed by Kline and McClintock [72].

Table 2.2. Uncertainty Data

Uncertainty	Error
Flow Rate, Q (for each reading)	± 2.0 %
Voltage supplied by power source, V	± 0.1 %
Current supplied by power source, I	± 0.1 %
Inlet temperature, T _i	± 0.1 °C
Electrical power, P	± 0.15 %
Heat transfer coefficient, h _{sp}	±11.8 %
Heat Flux, φ	±3.9%
Inner diameter, d _i	± 2 μm

According to this method, if an experimental result, r , is computed from J measured variables $X_{1...J}$, as follows;

$$r = r(X_1, X_2, \dots, X_J) \quad (12)$$

then the corresponding uncertainty in this experimental result is given by:

$$U_r^2 = \left(\frac{\partial r}{\partial X_1} \right)^2 U_{X_1}^2 + \left(\frac{\partial r}{\partial X_2} \right)^2 U_{X_2}^2 + \dots + \left(\frac{\partial r}{\partial X_J} \right)^2 U_{X_J}^2 \quad (13)$$

where U_r is the uncertainty in the result, U_{X_i} is the uncertainty in the variable X_i , etc.

3 RESULTS AND DISCUSSION

3.1 Results and Discussions on the Studies of Magnetic Actuation of Ferrofluids

3.1.1 Rectangular Rotor – Minitube Setup

The results of this first setup show a linear relationship between the angular velocity of the rectangular rotors and the volumetric flow rate as shown in Figure 8. The ferrofluid is subjected to a field that reaches a maximum magnetic field strength of 300mT. Figure 3.1. shows the relationship between the angular velocity and the volumetric flow rate.

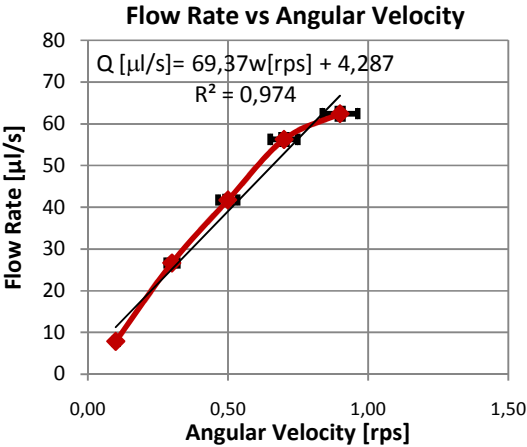


Figure 3.1. Flow rate vs angular velocity graph for rectangular rotor – minitube setup

The results show that achieving flow rates up to $60\mu\text{l/s}$ is possible with this design. If the angular velocity increases more than the maximum value, the average velocity of the nanofluid flow decreases because of the natural limitations of this design. More specifically, the magnetic field moves faster than the maximum steady state linear velocity of the fluid, and therefore, the fluid needs more than one cycle to move along a single length L . In addition to the above mentioned observations, when the rare earth magnet pair on the rotor moves faster than the limit velocity and is unable to drag the magnetized ferrofluid plug, the plug is reverted to the original position in the next cycle by the same magnet pair. Thus, the model is expected to break down at high

angular velocities, and the flow rate will be zero under such conditions. The limit for system to breakdown is 1.1 rps for minitube setups and 0.066 rps for microtube setups (both for rectangular and hexagonal setups).

Maximum volumetric flow rates that are achievable with the maximum applied magnetic field strengths are plotted in Figure 3.2. Since there is an absolute upper limit to the applicable magnetic field force, the distance between the magnet holders are adjusted to generate lower maximum magnetic field strengths.

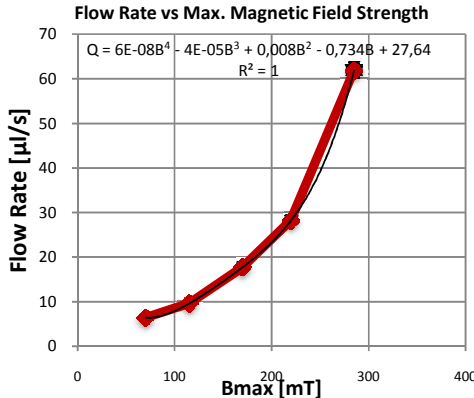


Figure 3.2. Max. flow rate vs max. magnetic field strength for rectangular rotor – minitube setup

The maximum flow rate values are obtained using a fixed angular velocity of 1 rps to ensure that the plotted curve only emphasizes on the relationship between magnetic field strength and flow rate.

The results from this setup suggest that the limit velocity for rotors can be increased by reducing the angle between the magnets. The skipping that causes the plug to revert could be prevented using this approach. This fact leads to the Hexagonal Rotor – Minitube design, which will be discussed in the following section.

3.1.2 Hexagonal Rotor – Minitube Setup

Decreasing the angle between the magnets reduces the severity of the sudden shifts in magnetic field, which creates magnetic dead zones and causes the limitation in terms of the flow rate values as mentioned before. The increased maximum achievable speed significantly improved the design and doubled the obtained flow rate values as shown in Figure 3.3.

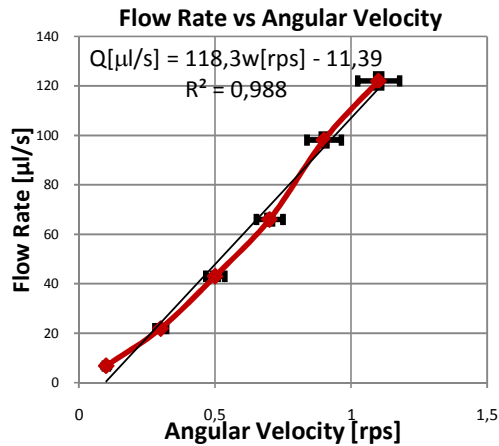


Figure 3.3. Flow rate vs angular velocity graph for hexagonal rotor – minitube setup

The relationship between the flow rate and angular velocity is again linear as expected, and flow rate values up to 120 μl/s can be obtained with this setup.

Figure 3.4. shows the relationship between the maximum magnetic field strength and maximum achievable flow rate. Accordingly, a flow rate of 120 μl/s can be achieved with a maximum magnetic field strength of 300 mT.

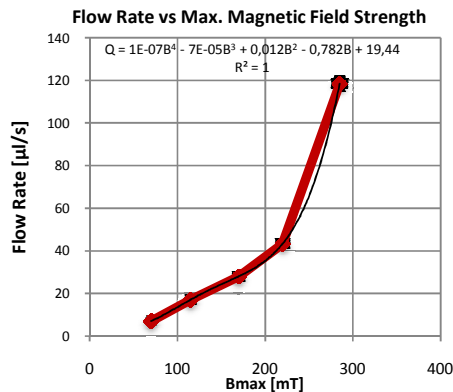


Figure 3.4. Max. flow rate vs max. magnetic field strength graph for hexagonal rotor setup

A commercial compact pump of similar size scale, which can also achieve the same flow rates as in the proposed design, was selected as an example. This pump constitutes the benchmark for comparison [76]. The commercial product, which is a single channel, variable speed compact pump, has the dimensions of 19 cm (length) x 8.9 cm (width) x 8.9 cm (height) and 1.42mm inner diameter of channel, whereas the proposed setups have the dimensions of 8cm (length) x 8cm (width) x 4cm (height), and

6cm (length) x 5cm (width) x 4cm (height), which are significantly smaller than the commercial pump in terms of its volume and has a 1.56 mm inner diameter channel(very close to the one in the commercial pump). It can be claimed that this proposed design is promising since it is more compact than the commercial pumps in terms of the size but generates the same flow rates compared to the compact commercial pumps. It should also be noted that these pumps can withstand significantly higher backpressures than the proposed pumps in this work (<250 Pa).In addition, another commercial micro pump, which is an Electroosmotic (EO) micropump (model 3000128 on datasheet) [77] with dimensions of 8mm (diameter) and 17.9mm (length), needs at least 460V of potential difference to generate the flow rate of the proposed design. This estimation was calculated by taking the referenced datasheet as is. The proposed design requires voltage values (few Volts) that are far below than this commercial micropump.

3.1.3 Rectangular Rotor – Microtube Setup

After successfully actuating ferrofluid plugs in minitubes, the next step was conducting experiments with microtubes by using the previously mentioned setups. First, the rectangular rotor setup was tested. It was seen that the design can also successfully actuate ferrofluid plugs in microtubes, but with proportionately lower flow rates. Figure 3.5. shows flow rates as a function of angular velocity, and the linear relationship between them is present similar to the minitube results.

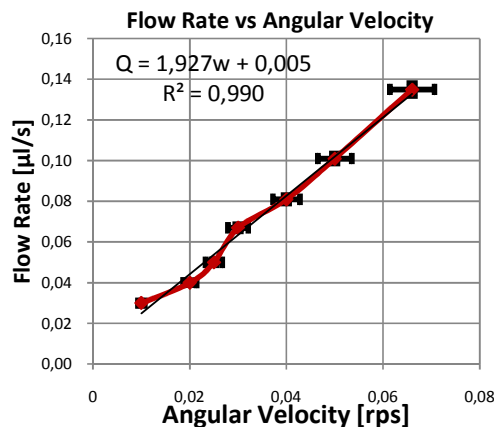


Figure 3.5. Flow rate vs angular velocity for rectangular rotor – microtube setup

Flow rates up to 0.135μl/s of are obtained with this design.

3.1.4 Hexagonal Rotor – Microtube Setup

Higher flow rates than the above mentioned setup was expected from this setup based on the improved results obtained from the first two setups that acted on minitubes. However, no significant improvement was recorded between results of this device and the previous device (Figure 3.6.).

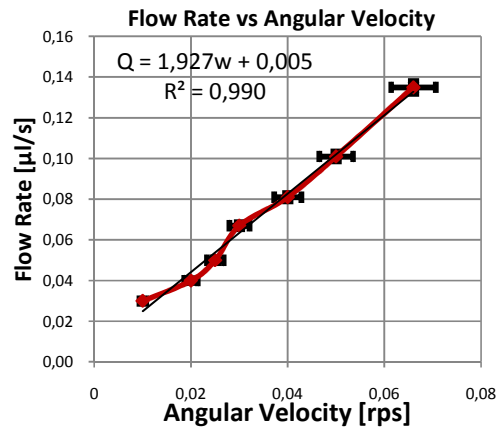


Figure 3.6. Flow rate vs angular velocity for hexagonal rotor – microtube setup

This shows that the previous device was fully capable of actuating the fluid at the maximum speed possible for the given tube size and magnetic field strength. To prevent skipping, the rotors rotate too slowly for the angle variation to have any significant effect. Any possible improvement is thus undetectable for this setup.

3.1.5 Conveyor Belt – Microtube Setup

The purpose of this design was inducing a continuous flow in addition to plug actuation. The proposed setup was successful in accomplishing this aim. Figure 3.7. shows the volumetric flow rate as a function of current fed to the system.

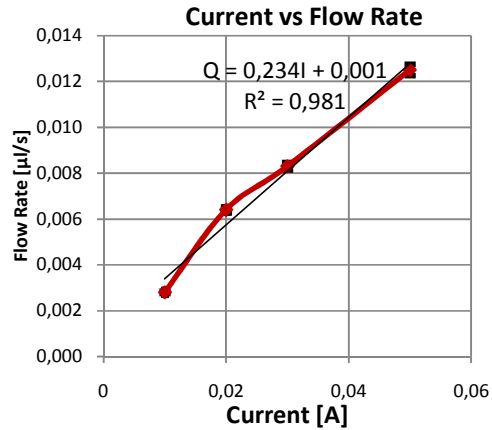


Figure 3.7. Current vs flow rate graph for conveyor belt set up

Flow rates up to $0.0125\mu\text{l/s}$ through a microtube with $254\mu\text{m}$ inner diameter can be obtained with this design. The flow is always expected to be fully laminar due to the length scale. The surface interactions have an improved effect with regard to body forces. This result shows that notable flow rates are achieved with modest power consumption especially since the magnetic field, which is interacting with the fluid, is not obtained through electrically induced magnetism. Instead of power losses due to the resistance of inductors, power consumption mostly occurs due to the viscous drag forces in the fluid, manipulation of magnetic interactions and various other mechanical inefficiencies related to the experimental setup. When compared to previous setups, this design has lower flow rate values, but this is compensated by the comparably lower power consumption and improvement of the flow by allowing continuous flow instead of plug actuation.

3.2 Results and Discussion of the Study of Heat Transfer Enhancement with Iron Oxide Based Ferrofluids

In Figures 3.8. and 3.9., experimental Nusselt numbers and ratios between theoretical results (obtained from commonly used correlations for laminar region $Re < 2300$ Shah and London [74], for turbulent region ($Re > 2300$) Dittus Bolter correlation with modifications due to developing flow effects [75]) and experimental Nusselt numbers are shown. Due to the short heated length, the flow is considered to be thermally developing. The thermal entrance length is around 14.8 cm for pure water at the lowest Reynolds number in this study justifying the use of correlations

recommended for thermally developing flows. It should be noted that for each flow rate there are multiple data points because of the change in thermophysical properties with increased heat flux values at the same flow rate (Fig. 3.8.). Since six data points were required for different heat fluxes at fixed flow rate, six Reynolds number values are present for each flow rate.

As can be seen from Figure 3.9., the existing widely used correlations could fairly predict the experimental data. For Reynolds numbers greater than 2300, the turbulent flow correlation (corresponding to flow rate of 1 ml/s and most of the experimental data points of the flow rate 0.62 ml/s) is taken, while the laminar flow correlation is employed for the experimental data corresponding to the flow rate of 0.36 ml/s. The above assumption made for the comparison is justified by the jump in experimental Nusselt number profile at $Re \sim 2200$ for the flow rate of 0.62 ml/s indicating sudden laminar flow-turbulent flow transition, which was also reported in the literature about single-phase flow in microtubes [78]. Almost all the experimental data fall within $\pm 30\%$ of theoretical values. This is in agreement with the reported results about single-phase flow in microtubes for both laminar and turbulent flows [79-80] and provides a validation for the experimental setup.

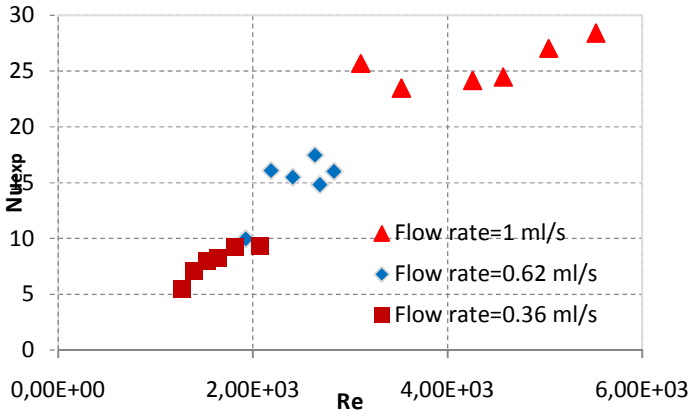


Figure 3.8. Experimental Nusselt number data for pure water

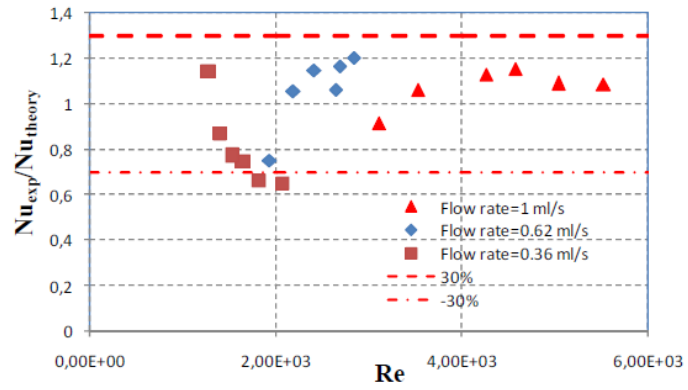
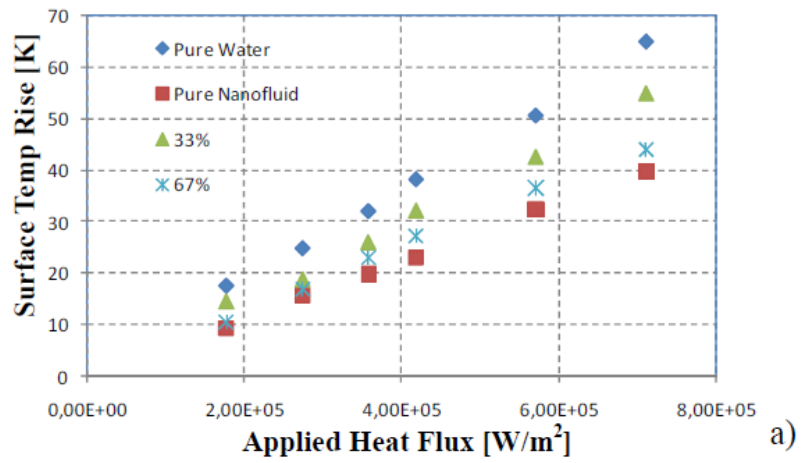
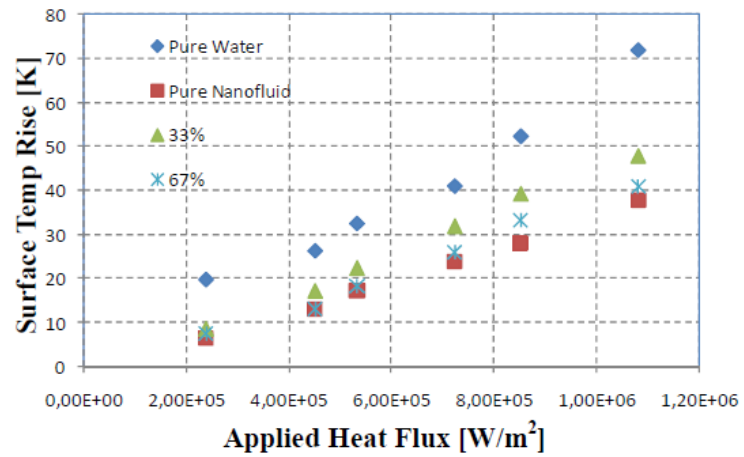


Figure 3.9. Comparison between the experimental data and existing theory for pure water



a)



b)

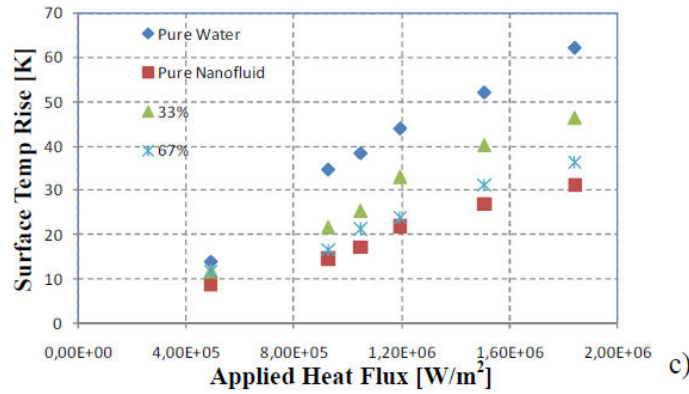


Figure 3.10. Surface temperature rise (with respect to ambient temperature) at a) $Q=0.36$ ml/s, b) $Q=0.62$ ml/s, c) $Q=1$ ml/s

In Figure 3.10., surface temperature rise at the exit of microtube is shown as a function of applied heat flux. A linear relationship between the applied heat flux and surface temperature rise exists as expected for single-phase fluid flows [81]. This relationship is observed under all the nanoparticle concentrations of the ferrofluid at all the flow rate values. The surface temperature rise at the outlet of the microtube increases to 31°C at a heat flux of ~ 184 W/cm^2 when high concentration ferrofluid (pure ferrofluid, $\sim 5\%$ volume fraction) is used as the coolant with the flow rate of 1 ml/s. When the high concentration ferrofluid is diluted by 33%, the temperature rise increases to 36°C . A further dilution of the ferrofluid results in a maximum increase of 46.1°C , which proves that the heat removal capability decreases with dilution. A surface temperature rise of 62.1°C can be observed during the experiments with pure water at maximum applied heat flux (~ 184 W/cm^2). The same trend is consistently observed with lower flow rates. In addition, with decreasing flow rate the surface temperature rise increases at the same applied power values for all the samples due to diminishing convective effects. For the flow rates of 0.62 ml/s and 0.36 ml/s, the surface temperature rises are 71.9°C and 64.8°C with pure water at maximum applied heat fluxes of 108 W/cm^2 and 71 W/cm^2 , respectively, while the surface temperature rises become 37.8°C and 39.9°C for the high concentration nanofluid, respectively. The decrease of around 100% in the maximum surface temperature (exit of the microtube) with the high concentration nanofluid at significant heat fluxes (>100 W/cm^2) reveals the potential of the use of ferrofluids in micro scale cooling applications.

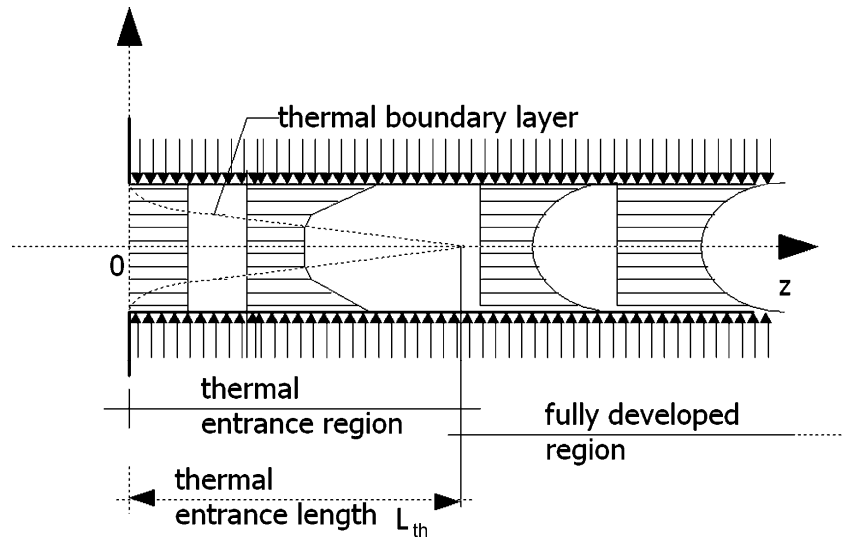
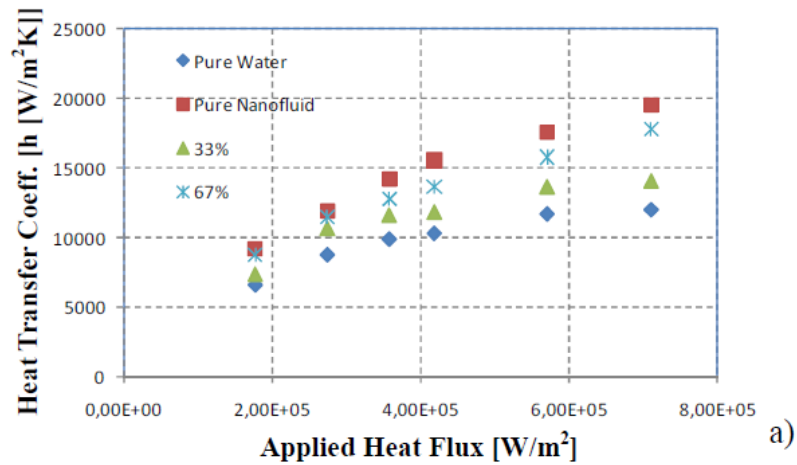


Figure 3.11. Thermally developing flow [82]

As previously mentioned; due to the short heated length, which is 2.5 cm, the flow is considered to be thermally developing. Since for pure water at the lowest Re , the thermal entrance length is around 14.8 cm, the heat transfer coefficient profiles obtained from this study stays within the thermally entrance region as can be seen in Figure 3.11.



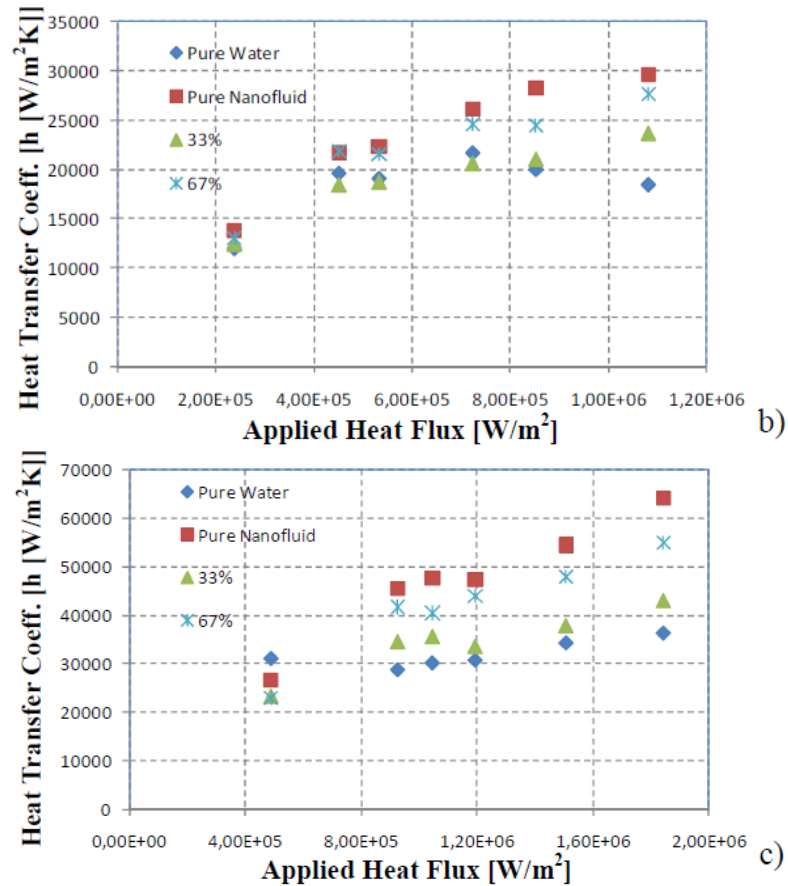


Figure 3.12. Heat transfer coefficients as a function of applied heat flux at a) $Q=0.36$ ml/s, b) $Q=0.62$ ml/s, c) $Q=1$ ml/s

Heat transfer coefficient profiles which are obtained from the commonly used correlations [74-75] and the experimental results from the obtained surface and outlet temperature data are shown in Figure 3.12. for different flow rates. An increasing trend in heat transfer coefficient with flow rate could be recognized for all the fluid samples used in the current study. For the laminar flow portion of the experimental data ($Re < 2300$ classified for water, flow rates < 1 ml/s for other working fluids), the reason is due to the developing flow conditions, where Nusselt number is dependent on Reynolds number [74]. In the turbulent flow portion, Nusselt number is strongly dependent on Reynolds number, which is also coupled with developing flow effects. As a result, higher heat transfer coefficients are attained at larger flow rates as expected. All the ferrofluid samples used in the current study demonstrate the same trend. However, the differences in heat transfer coefficients between pure fluid and ferrofluid samples are not as much as in surface temperature rise. This is due to the lower exit fluid temperatures in ferrofluid samples resulting from higher specific heat and density values

in ferrofluid samples [83]. As a result, smaller differences in heat transfer coefficients compared to surface temperature differences are present between pure water and ferrofluid samples.

As seen from Figures 3.12 and 3.13., the enhancement in convective heat transfer grows with increasing nanoparticle concentration. The average enhancement in heat transfer coefficients is 46.5%, 34.5%, and 16.5% for the high concentration ferrofluid sample, the ferrofluid sample diluted by 33%, and the ferrofluid sample diluted by 67% at the flow rate of 0.36 ml/s, respectively. For all the working fluids, laminar flow conditions occur at this flow rate. At the flow rate of 0.62 ml/s, the enhancements decrease to 27.5%, 19.7%, and 4.1% for the high concentration ferrofluid sample, the ferrofluid sample diluted by 33%, and the ferrofluid sample diluted by 67%, respectively. The decrease in heat transfer coefficient enhancement could be attributed to the existence of turbulent flow conditions for the most of the experimental data during the experiments with pure water at this flow rate. In the literature, sudden transitions from laminar to turbulent flows were reported at $Re \sim 2000$ for microtubes [72, 80]. Due to higher viscosities in ferrofluid samples, the transition to turbulent flow occurs at higher flow rates so that heat transfer enhancements become lower due to the still existing laminar flow conditions for the ferrofluid samples. Turbulent flow conditions are expected for the experiments with all the nanofluid samples at the flow rate of 1ml/s in addition to the pure water experiments, which generates an increase in heat transfer enhancements. Thus, increased convective heat transfer enhancement due to nanoparticle motion under high speed flows and subsequent additional mixing provided by nanoparticles contributes to the heat transfer performance [84]. Accordingly, the average increases in heat transfer coefficients are 61.2%, 43.3%, and 15.1% for the high concentration ferrofluid sample, the ferrofluid sample diluted by 33%, and the ferrofluid sample diluted by 67%, respectively.

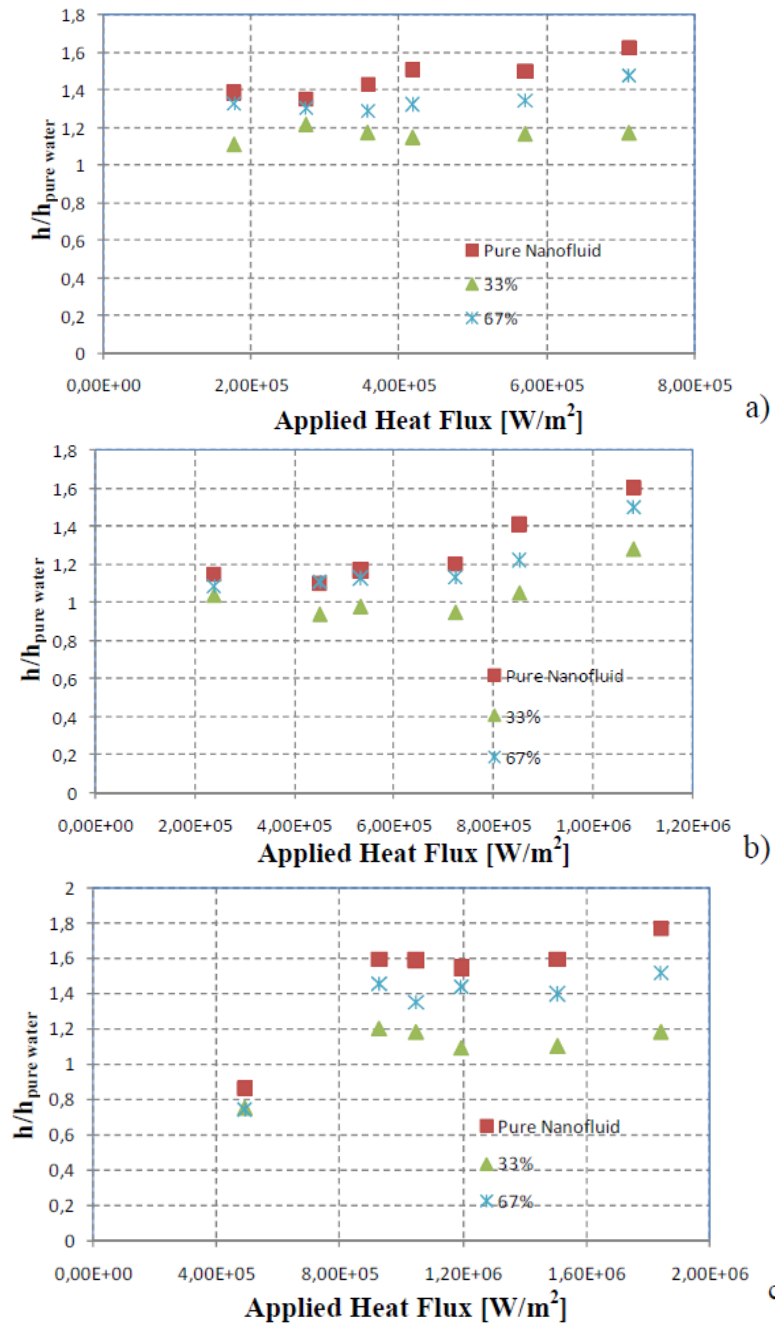


Figure 3.13. Heat transfer coefficient enhancement ($h/h_{\text{pure water}}$) at a) $Q=0.36 \text{ ml/s}$, b) $Q=0.62 \text{ ml/s}$, c) $Q=1 \text{ ml/s}$

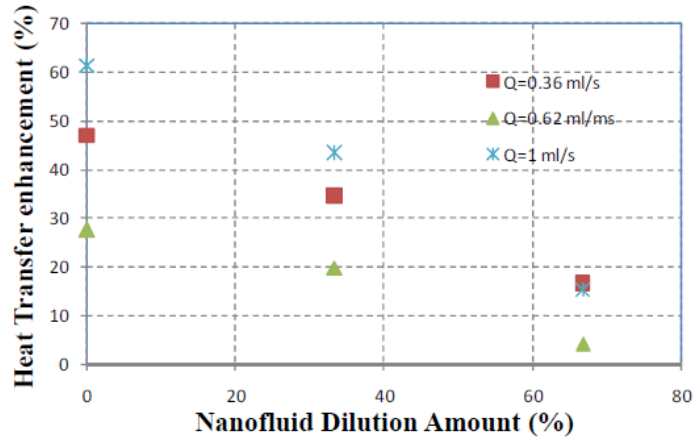


Figure 3.14. Heat transfer enhancement (in %) (the average enhancement in heat transfer coefficients) as a function of dilution amount (with respect to the high concentration nanofluid)

As seen from Figure 3.14., there is no clue for saturation in heat transfer coefficient profiles with increasing volume fraction over the volume fraction range in this study (0%-5%), although the upper range for volume fraction overlaps with volume fractions, beyond which saturation or decrease in heat transfer was reported in the literature [85-87]. The lack of saturation could be explained by the improved stability in nanoparticle suspension with Lauric acid coating so that any agglomeration/deposition of particles with increased volume fraction and sudden contraction in flow passage caused by the inlet of microtube could be avoided and the positive effect of nanoparticle concentration could be extended to high volume fraction values (>3%). In addition, ferromagnetic nanoparticles could be actuated inside a nanofluid with magnetic fields so that for the heat transfer enhancement from the surface is possible. In previous studies, it was shown that flow velocities greater than 1 cm/s were achievable in mini/micro scale at decent magnetic fields (<0.3mT) without any external source [88]. In another study [89], it was shown that an average heat transfer coefficient enhancement of 37.5% was achieved with magnetic actuation of ferrofluids inside a pool with 5W of additional power consumption. Thus, there is a strong possibility for improving the heat transfer performance of ferrofluids with external means such as magnetic fields, which will be considered as future work by the authors. Moreover, the ease in their fabrication method allows their preparation in large quantities.

Better heat transfer properties may certainly improve the utility of ferromagnetic nanoparticles in biomedical treatments (e.g. tumor ablation with improved local heat transfer). Minimal agglomeration/deposition and lack of saturation are desired

properties to avoid clogging of tissue capillary vessels that can be as narrow as 5-10 μm in diameter. These properties might allow particles access into deeper regions of diseased tissues, hence lead to better and more efficient targeted treatments. All these properties of SPIO-LA particles make them ideal candidates for improved heat transfer treatment tools. Further biological studies in cellular and animal models of human disease will reveal their true potential in biomedical treatments.

All of these advantages strengthen the potential of the use of Iron Oxide Nanoparticle based ferrofluids as new generation coolants and drug carrier agents.

4 CONCLUSION

4.1 Conclusions of the Studies of Magnetic Actuation of Iron Oxide Based Ferrofluids

In the first studies, methods to actuate ferrofluids with varying magnetic fields were tested. The methods of composing a magnetic field with rotating magnetic field sources to obtain a linearly moving magnetic gradient were successful. The generated magnetic fields actuated the ferrofluid plugs in mini and microtubes. Flow rates up to $120\mu\text{l/s}$ and $0.135\mu\text{l/s}$ were achieved in the experiments in minitubes and microtubes with modest maximum magnetic field magnitudes of 300mT for discontinuous and continuous actuation, respectively. A simple comparison of results shows that the ratios of flow rates are consistent with the physical scale ratio of minitubes and microtubes.

It was proven that actuation of ferrofluid plugs in microtubes with very modest power rates is possible, if permanent magnets with high magnetic moment density are employed as the field sources. These devices do not produce waste heat like electrically generated fields, and they always remain “on” in the last functioning state if the power is cut. The lack of generated heat reduces the unwanted interference with the fluid and tubing.

It was previously seen that when a series of rotating magnets are employed to simulate a translating magnet, reducing the angular difference of consequent magnets improves the quality of the resultant magnetic field. The said improvement was significant in actuation of ferrofluids in minitubes. The errors in the magnetic field were dampened and the average velocity of the plug was increased. However, the results obtained from modified devices that operate in microtubes showed that the aforementioned adjustment to the angular displacement between magnets is irrelevant in microscale. For this reason, results for hexagonal rotor and rectangular rotor designs were almost identical in micro scale.

Continuous flows of ferrofluids could be also generated with a conveyor belt system. Flow rates up to $0.0125\mu\text{l/s}$ through microtubes could be obtained with the proposed approach.

The promising results suggest that ferrofluids merit more research efforts in micro pumping, and magnetic actuation could have a high potential for being a significant alternative for more common techniques such as electromechanical, electrokinetic, and piezoelectric actuation.

4.2 Conclusions of the Study of Heat Transfer Enhancement with Iron Oxide Based Ferrofluids

The second study presents experimental results on convective heat transfer performances of ferrofluid samples at different iron-oxide based nanoparticle concentrations, applied heat fluxes and flow rates after a validation study with pure water as the working fluid. The results suggest that using ferrofluids as heat transfer fluids is a strong and feasible alternative due to their enhanced heat transfer performances, easy preparation methods.

Moreover, they could be synthesized in large quantities and have improved stability with Lauric acid coating avoiding any agglomeration and deposition. Smaller nanoparticle sizes of ferrofluids prevent clogging of the minichannels during heat transfer, which also enables the miniaturization of the systems.

A decrease of around 100% in the maximum surface temperature (exit of the microtube) with the ferrofluid compared to pure water at significant heat fluxes ($>100 \text{ W/cm}^2$) was recorded. It was also observed that the enhancement in heat transfer increases with nanoparticle concentration in the absence of saturation in heat transfer coefficient profiles. These promising results in terms of heat transfer properties and improved stability offer significant advantages of iron oxide based ferrofluids in heat transfer, drug delivery and biological applications.

4.3 Contribution to the Scientific Knowledge

Micropumps are one of the most important and popular microfluidic systems. This thesis contributes to the literature by presenting the behavior of ferrofluid under dynamic magnetic fields in mini/micro channels so that efficient actuation methods can be developed for micropumping purposes. The devices designed, implemented and

presented in this thesis provide alternatives to the literature in terms of external and contactless actuation method, applicable to the numerous areas such as valving sealing lab-on-chip applications, low-cost but very efficient devices with large displacement capabilities, high forces, fast response time and ease of implementation and most importantly higher flow rates than the existing pumps even some commercialized ones [76-77]. It can be claimed that this proposed design is promising since it is more compact than the commercial pumps in terms of the size but generates the same flow rates compared to the compact commercial pumps. It should also be noted that these pumps can withstand significantly higher backpressures than the proposed pumps in this work (<250 Pa). In addition, another commercial micro pump, which is an Electroosmotic (EO) micropump (model 3000128 on datasheet) [77] with dimensions of 8mm (diameter) and 17.9mm (length), needs at least 460V of potential difference to generate the flow rate of the proposed design. This estimation was calculated by taking the referenced datasheet as is. The proposed design requires voltage values (few Volts) that are far below than this commercial micropump.

Heat transfer in microchannels has become progressively important with the rapid development of microelectronic devices and micro manufacturing technology, since microchannel heat exchangers and evaporators present several advantages, such as reduced size, higher thermal efficiency and low fluid inventory. This thesis contributes to the literature by analyzing the heat transfer enhancement capability of ferrofluids, which are a type of the new generation nanofluids. A decrease of around 100% in the maximum surface temperature (exit of the microtube) with iron-oxide nanoparticle based ferrofluids compared to pure water at significant heat fluxes ($>100 \text{ W/cm}^2$) was recorded. It was also observed that the enhancement in heat transfer increases with nanoparticle concentration in the absence of saturation in heat transfer coefficient profiles. These promising results in terms of heat transfer properties and improved stability offer significant advantages of iron oxide nanoparticle based ferrofluids in heat transfer in many different areas such as microelectronics, drug delivery and biological applications.

REFERENCES

- [1] Van Lintel H.T.G., Van de Pol F.C.M., Bouwstra S., 1988, "A piezoelectric micropump based on micromachining of silicon.", *Sens Actuators*, 15:153–167.
- [2] Yamahata C., Chastellain M., Parashar V.K., Petri A., Hofmann H., Gijs M.A.M., 2005, "Plastic micropump with ferrofluidic actuation.", *J Microelectromech Syst*, 14(1):96–102.
- [3] Woias P., 2004, "Micropumps-past, progress and future prospects.", *Sens Actuators B*, 105:28–38.
- [4] Anton I., Vekas L., Potencz I., Suciuc E., 1980, "Ferrofluid flow under the influence of rotating magnetic fields.", *IEEE Trans Magn*, 16:283–287.
- [5] Leland, J.E., 1991, "Ferrofluid piston pump for use with heat pipes or the like.", U.S. patent, 5 005 639.
- [6] Greivell N.E., Hannaford B., 1997, "The design of a ferrofluid magnetic pipette.", *IEEE Trans Biomed Eng*, 44(3):129–135.
- [7] Pe´rez-Castillejos R., Plaza J.A., Esteve J., Losantos P., Acero M.C., Cane C., Serra-Mestres F., 2000, "The use of ferrofluids in micromechanics.", *Sens Actuators A*, 84:176–180.
- [8] Hartshorne H., Backhouse C.J., Lee W.E., 2004, "Ferrofluid-based microchip pump and valve.", *Sens Actuators B*, 99:592–600.
- [9] Hatch A., Kamholz A.E., Holman G., Yager P., Bohringer F.K., 2001, "A ferrofluidic magnetic micropump.", *J Microelectromech Syst*, 10(2):1.
- [10] Al-Halhouli A.T., Kilani M.I., Buttgenbach S., 2010, "Development of a novel electromagnetic pump for biomedical applications.", *Sens Actuators A*, 162:172–176.
- [11] Kong T.F., Shin H., Sugiarto H.S., Liew H.F., Wang X., Lew W.S., Nguyen N.T., Chen Y., 2011, "An efficient microfluidic sorter: implementation of double meandering micro striplines for magnetic particles switching.", *Microfluid Nanofluid*, 10:1069–1078.
- [12] Jin X., Aluru N.R., 2011, "Gated transport in nanofluidic devices. *Microfluid Nanofluid*.", doi:10.1007/s10404-011-0796-3.
- [13] Zhang R., Dalton C., Jullien G.A., 2011, "Two-phase AC electrothermal fluidic pumping in a coplanar asymmetric electrode array.", *Microfluid Nanofluid*, 10:521–529.

- [14] Sanders G.H.W., Manz A., 2000, "Chip- based microsystems for genomic and proteomic analysis.", *Trends in Analytical Chemistry*, 19(6):364–378.
- [15] Chen H., Abolmatty A., Faghri M., 2011, "Microfluidic inverse phase ELISA via manipulation of magnetic beads.", *Microfluid Nanofluid*, 10:593–605.
- [16] Martsenyuk M.A., 1980, "A dissipative process in ferrofluid in nonhomogenous magnetic field.", *IEEE Trans Magn*, 16:298–300.
- [17] Kakac S., Pramuanjaroenkij A., 2009, "Review of convective heat transfer enhancements with nanofluids.", *Int J Heat Mass Transf*, 52:3187–3196.
- [18] Acar H.Y., Garaas R.S., Syud F., Bonitatebus P., Kulkarni A.M., 2005, "Superparamagnetic nanoparticles stabilized by polymerized PEGylated coatings.", *J Magn Magn Mater*, 293:1–7.
- [19] Pamme N., 2006, "Magnetism and microfluidics.", *Lab Chip* 6:24–38.
- [20] Zhu T., Cheng R., Mao L., 2011, "Focusing microparticles in a microfluidic channel with ferrofluids.", *Microfluid Nanofluid*, doi:10.1007/s10404-011-0835-0.
- [21] Dababneh M.S., Ayoub N.Y., 1995, "The effect of Oleic Acid on the stability of magnetic ferrofluid.", *IEEE Trans on Magn*, 31:4178–4180.
- [22] Ando B., Baglio S., Beninato A., 2009, "Non-invasive implementation of pumping mechanism in pre-existing capillary.", *IEEE Sensors Conference*.
- [23] Derec C., Wilhelm C., Servais J., Bacri J.C., 2010, "Local control of magnetic objects in microfluidic channels.", *Microfluidics Nanofluidics*, 8:123–130.
- [24] Tsai K.L., Pickard D., Kao J., Yin X., Leen B., Knutson K., Kant R., Howe R.T., 2009, "Magnetic nanoparticle-driven pumping in microchannels.", *Transducers*, Denver, CO, USA.
- [25] Afshar R., Lehnert T., Moser Y., Gijs M.A.M., 2009, "Magnetic particle dosing, release and separation in a microfluidic chip with magnetic actuation.", *International Solid-State Sensors, Actuators and Microsystems Conference*, Denver, CO, USA.
- [26] Wang Y., Zhao Y., Cho S.K., 2007, "In-droplet magnetic beads concentration and separation for digital microfluidics.", *The 14th international conference on solid-state sensors, actuators and microsystems, Transducers and Eurosensors'07*, Lyon, France.
- [27] Song W., Ding Z., Son C., Ziaie B., 2007, "A dynamic ferrofluid platform for micromanipulation", *MEMS 2007*, Kobe, Japan.
- [28] Lien K.Y., Liu C.J., Lin Y.C., Kuo P.L., Lee G.B., 2009, "Extraction of genomic DNA and detection of single nucleotide polymorphism genotyping utilizing an

- integrated magnetic bead-based microfluidic platform.”, *Microfluid Nanofluid*, 6:539–555.
- [29] Lacharme F., Vandevyer C., Gijss M.A.M., 2009, “Magnetic beads retention device for sandwich immunoassay: comparison of offchip and on-chip antibody incubation.”, *Microfluid Nanofluid*, 7:497.
- [30] Chen Y.A., Huang Z.W., Tsai F.S., Chen C.Y., Lin C.M., Wo A.M., 2011, “Analysis of sperm concentration and motility in a microfluidic device.”, *Microfluid Nanofluid*, 10:59–67.
- [31] Ando B., Salvatore B., Beninato A., 2011, “An IR methodology to assess the behavior of ferrofluidic transducers case of study: a contactless driven pump.”, *IEEE Sens J*, 11:1.
- [32] Tierno P., Golestanian R., Pagonabarraga I., Sagues F., 2008, “Controlled swimming in confined fluids of magnetically actuated colloidal rotors.”, *Phys Rev Lett*, 101:21830–21834.
- [33] Sing C.E., Schmid L., Schneider M.F., Franke T., Alexander-Katz A., 2010, “Controlled surface-induced flows from the motion of selfassembled colloidal walkers.”, *PNAS*, 107:535–540.
- [34] Karle M., Wohrle J., Miwa J., Paust N., Roth G., Zengerle R., Stetten F., 2010, “Controlled counter-flow motion of magnetic bead chains rolling along microchannels.”, *Microfluid Nanofluid*, 10:935–939.
- [35] Maxwell, J.C., 1881, “A Treatise on Electricity and Magnetism.”, Clarendon Press, Oxford, UK, second edition.
- [36] Keblinski P., Phillpot S.R., Choi S.U.S., Eastman, J.A., 2002, “Mechanisms of heat flow in suspensions of nano-sized particles (nanofluids).”, *International Journal of Heat and Mass Transfer*, 45, 855–863.
- [37] Ding Y., Wen, D., 2005, “Particle migration in a flow of nanoparticle suspensions.”, *Powder Technology*, 149, no. 2-3, 84–92.
- [38] Khaled A.R.A., Vafai K., 2005, “Heat transfer enhancement through control of thermal dispersion effects.”, *International Journal of Heat and Mass Transfer*, 48, no. 11, 2172.
- [39] Colla L., Fedele L., Scattolini M., Bobbo S., 2011, “Water-Based Fe₂O₃ Nanofluid Characterization: Thermal Conductivity and Viscosity Measurements and Correlation”, Hindawi Publishing Corporation, *Advances in Mechanical Engineering*, Volume 2012, Article ID 674947.

- [40] Choi, S.U.S., 1995, “Enhancing thermal conductivity of fluids with nanoparticles.”, *Developments and Applications of Non-Newtonian Flows*, FED-Vol. 231/MD-Vol. 66, 99–105.
- [41] Eastman, J.A., Choi, S.U.S, Li, S., Yu, W., Thompson, L.J., 2001, “Anomalously increased effective thermal conductivities of ethylene glycol-based nanofluids containing copper nanoparticles,” *Appl. Phys. Lett.* **78**, 718.
- [42] Choi, S.U.S, Zhang, Z.G., Yu, W., Lockwood, F.E., Grulke, E.A., 2001, “Anomalous thermal conductivity enhancement in nanotubes suspensions”, *Appl. Phys. Lett.* **79**, 2252.
- [43] Xuan Y., Li, Q., 2000, “Heat transfer enhancement of nanofluids,” *Int. J. Heat Fluid Flow* **21**, 58.
- [44] Xuan Y., Roetzel, W., 2000, “Conceptions for heat transfer correlation of nanofluids,” *Int. J. Heat Mass Transfer* **43**, 3701.
- [45] Das S. K., Putta N., Thiesen P., Roetzel, W., 2003 , “Temperature dependence of thermal conductivity enhancement for nanofluids.”, *ASME Trans. J. Heat Transfer*, 125, 567–574.
- [46] Jang S. P., Choi S. U. S., 2004 , “Role of Brownian motion in the enhanced thermal conductivity of nanofluids.”, *Applied Physics Letters*, 84, 4316–4318.
- [47] Maiga S. E. B., Cong Tam N., Galanis N., Roy G., Mare T., Coqueux M., 2006 , “Heat transfer enhancement in turbulent tube flow using Al₂O₃ nanoparticle suspension.”, *International Journal of Numerical Methods for Heat and Fluid Flow*, 16, no. 3, 275–292.
- [48] Abu-Nada E., 2008, “Application of nanofluids for heat transfer enhancement of separated flows encountered in a backward facing step.”, *International Journal of Heat and Fluid Flow*, 29, no. 1, 242–249.
- [49] Wong K.V., De Leon O., 2010, “Applications of Nanofluids: Current and Future”, *Advances in Mechanical Engineering*, Article ID 519659, doi:10.1155/2010/519659.
- [50] Shen B., Shih A. J., Tung S.C., Hunter M., “Application of nanofluids in minimum quantity lubrication grinding,” *Tribology and Lubrication Technology*.
- [51] Tzeng S.C., Lin C.W., Huang K.D., 2005, “Heat transfer enhancement of nanofluids in rotary blade coupling of four-wheel-drive vehicles,” *Acta Mechanica*, 179, no. 1-2, pp. 11–23.

- [52] Olaru R., Pal C., Petrescu C., 2001, “Current to pressure transducer with magnetic fluid”, *Sensors and Actuators A*, 91, 150-152.
- [53] Roy G., Nguyen C.T., Lajoie P.R., 2004, “Numerical investigation of laminar flow and heat transfer in a radial flow cooling system with the use of nanofluids.”, *Superlattices and Microstructures*, 35, 497–511.
- [54] Park K.J., Jung, D., 2007, “Boiling heat transfer enhancement with carbon nanotubes for refrigerants used in building air-conditioning.”, *Energy and Buildings*, 39, 1061–1064.
- [55] Shawgo R.S., Grayson A.C.R., Li Y., Cima M.J., 2002, “BioMEMS for drug delivery,” *Current Opinion in Solid State and Materials Science*, 6, no. 4, pp. 329–334.
- [56] Ma H. B., Wilson C., Borgmeyer B., 2006, “Effect of nanofluid on the heat transport capability in an oscillating heat pipe,” *Applied Physics Letters*, 88, no. 14, Article ID 143116, 3 pages.
- [57] Nguyen C.T., Roy G., Gauthier C., Galanis N., 2007 , “Heat transfer enhancement using Al₂O₃-water nanofluid for an electronic liquid cooling system,” *Applied Thermal Engineering*, 27, no. 8-9, pp.1501–1506.
- [58] Xuan Y., Li Q., Ye M., 2007, “Investigations of convective heat transfer in ferrofluid microflows using lattice-Boltzmann approach. *Int J Therm Sci*;46:105–111.
- [59] Melikhov Y., Lee S.J., Jiles D.C., Schmidt D.H., Porter M.D., Shinar R., 2003, “Microelectromagnetic ferrofluid-based actuator.”, *J Appl Phys*;93:8438–8440.
- [60] Nethe A., Schoppe T., Stahlmann H., 1999, “Ferrofluid driven actuator for a left ventricular assist device.”, *J Magnet Magnet Mater*;201:423–426.
- [61] Love L.J., Jansen J.F., Mcknight T.E., Roh Y., Phelps T.J., Yeary L.W., Cunningham G.T., 2005, “Ferrofluid field induced flow for microfluidic applications.”, *IEEE Trans Mechatron*;10:68–76.
- [62] Eastman J.A., Choi S.U.S., Li S., Soyez G., Thompson L.J., Di Melfi R.J., 1999 , “Novel thermal properties of nanostructured materials”, *Mater. Sci. Forum*, 312-314, 629-634.
- [63] Lee S., Choi S.U.S., Li S., Eastman J.A., 1999 , “Measuring thermal conductivity of fluids containing oxide nanoparticles”, *ASME Journal of Heat Transfer*, 121, 280-289.
- [64] Scherer C., Neto A.M.F., 2005, “Ferrofluids: Properties and Applications”, *Brazilian Journal of Physics*, 35, no. 3A, September.
- [65] Bilgin A., Kurtoglu E., Erk H.C., Sesen M. Yagci Acar H.F., Kosar A., 2011, “Magnetic nanoparticle based nanofluid actuation with dynamic magnetic fields”,

ASME 2011 9th International Conference on Nanochannels, Microchannels, and Minichannels, ICNMM 9, Edmonton, Canada, June 19-22, ICNMM2011-58222.

[66] Bilgin A., Kurtoglu E., Erk H.C., Sesen M., Yagci Acar H.F., Kosar A., 2011, “A novel magnetomechanical pump to actuate ferrofluids in minichannels”, Thermal and Material Nonoscience and Nanotechnology, TMNN-2011, Antalya, Turkey, May 29-June 3.

[67] Tietze R., Lyer S., Durr S., Alexiou C., 2012, “Nanoparticles for cancer therapy using magnetic forces”, *Nanomedicine (Lond)*. 7(3):447-57.

[68] Veeramachaneni U.K., Carroll R.L., 2007, Excerpt from the Proceedings of the COMSOL Conference, Boston, MA.

[69] Choi H.S., Kim Y.S., Kim K.T., Park I.H., 2008, “Simulation of hydrostatical equilibrium of ferrofluid subject to magneto-static field.”, *IEEE Trans Magn*, 44:818–821.

[70] Menz A., Benecke W., Perez-Castillejos R., Plaza J.A., Esteve J., Garcia N., Higuero J., Diez-Caballero T., 2000, “Fluidic components based on ferrofluids.”, 1st annual international IEEE-EMBS special topic conference on microtechnologies in medicine and biology, Lyon, France.

[71] Mao L., Koser H., 2011, “An integrated MEMS ferrofluid pump using insulated metal substrate.”, 31st Annual conference of IEEE, IECON, pp 2372–2375.

[72] Kline S., McClintock F.A., 1953, “Describing Uncertainties in Single-Sample Experiments.”, *Mech Eng (Am Soc Mech Eng)* 75:3–8.

[73] GUM (Guide to the Expression of Uncertainty in Measurement)-ISO, 1995, (with minor corrections), “Evaluation of measurement data—Guide to the expression of uncertainty in measurement.”, Joint Committee for Guides in Metrology (JCGM), 100:2008.

[74] Shah R.K., London A.L., 1978, “Laminar flow forced convection in ducts”, Academic Press, New York.

[75] Incropera F.P., DeWitt C.P., 1996, “Fundamentals of Heat and Mass Transfer”, John Wiley, New York.

[76] Single-Channel Variable-Speed Compact Commercial Pumps, Retrieved from http://www.masterflex.com/catalog/product_view.asp?sku=7712020.

[77] Electroosmotic (EO) micropump model 3000128 on datasheet, Retrieved from http://www.dolomitmicrofluidics.com/images/PDFs/micro_elctro_osmotic_pump.pdf.

- [78] Guo Z.Y., Li Z.X., 2003, "Size effect on microscale single-phase flow and heat transfer", *International Journal of Heat and Mass Transfer*, 46, 149–159.
- [79] Morini G.L., 2004, "Single-phase convective heat transfer in microchannels: a review of experimental results", *International Journal of Thermal Sciences*, 43, 631–651.
- [80] Ozdemir M.R., Kosar A., "Experimental study on single-phase flow in microtubes at High Mass Flow rates", *Journal of Heat Transfer*, Accepted.
- [81] Qu W., Mudawar I., 2002, "Experimental and numerical study of pressure drop and heat transfer in a single-phase micro-channel heat sink", *International Journal of Heat and Mass Transfer*, 45, Issue 12, Pages 2549-2565, ISSN 0017-9310, 10.1016/S0017-9310(01)00337-4.
- [82] Li, D., (Ed.), 2008, "Encyclopedia of microfluidics and nanofluidics", Springer.
- [83] Wang X.Q., Mujumdar A. S., 2008, "A review on nanofluids- Part 1: Theoretical and numerical investigations", *Brazilian Journal of Chemical Engineering*, 25, No. 04, pp. 613 - 630, October - December.
- [84] Buongiorno J., 2006, "Convective transport in nanofluids.", *Journal of Heat Transfer*, 128, 240–250.
- [85] Bozhko A. A., Putin G. F., 2004, "Magnetic action on convection and heat transfer in ferrofluid", *Indian Journal of Engineering & Material Sciences*, 11, pp. 309-314.
- [86] Mohammadpourfard M., 2012, "Numerical Study of Ferrofluid Flow and Heat Transfer in the Presence of a Non-uniform Magnetic Field in Rectangular Microchannels", *Heat Transfer—Asian Research*, 41 (4).
- [87] Martin-Callizo C., Palm B., Ali R., 2007, "New experimental results on flow boiling of R-134a in a vertical microchannel", *The 10th UK National Heat Transfer Conference*, September 10-11, Edinburgh, UK.
- [88] Kurtoglu, E., Bilgin, A., Sesen, M., Mısırlıoğlu, B., Yıldız, M., Yagci, Acar, H. F. Y., Kosar, A., 2012, "Ferrofluid actuation with varying magnetic fields for micropumping applications", *Microfluid Nanofluid*, 13:683–694.
- [89] Sesen, M., Teksen, Y., Sendur, K., Menguc, M. P., Ozturk, H., Acar, H.F.Y., Kosar, A., 2012, "Heat transfer enhancement with actuation of magnetic nanoparticles suspended in a base fluid", *J. Appl. Phys.*, 112, 064320.